Emission inventory of air pollutants and chemical speciation for specific anthropogenic sources based on local measurements in the Yangtze River Delta region, China

Jingyu An[1,2], Yiwei Huang[1], Cheng Huang[1,*], Xin Wang[3], Rusha Yan[1], Qian Wang[1], Hongli Wang[1], Sheng'ao Jing[1], Yan Zhang[2], Yiming Liu[2], AJ Yuan Chen[4], Chang Xu[1], Liping Qiao[1], Min Zhou[1], Shuhui Zhu[1], Qingyao Hu[1], Jun Lu[1], Changhong Chen[1]

1. State Environmental Protection Key Laboratory of the Formation and Prevention of Urban Air Pollution Complex, Shanghai Academy of Environmental Sciences, Shanghai 200233, China

2. Shanghai Key Laboratory of Atmospheric Particle Pollution and Prevention, Department of Environmental Science and Engineering, Fudan University, Shanghai 200438, China

3. China National Environmental Monitoring Centre, Beijing 100012, China

4. University of Southern California, Los Angeles, CA 90089, USA

Abstract: A high-resolution air pollutant emission inventory for the Yangtze River Delta (YRD) region was updated for 2017 using emission factors and chemical speciation based mainly on local measurements in this study. The inventory included 424 non-methane volatile organic compounds (NMVOC) and 43 fine particulate matter ($PM_{2.5}$) species from 259 specific sources. The total emissions of SO_2, NO_x, CO, NMVOCs, PM_{10}, $PM_{2.5}$, and NH_3 in the YRD region in 2017 were 1,552, 3,235, 38,507, 4,875, 3,770, 1,597, and 2,467 Gg respectively. SO_2 and CO emissions were mainly from boilers, accounting for 49% and 73% of the total. Mobile sources dominated NO_x emissions contributing 57% to the total. NMVOC emissions, mainly from industrial sources, made up 61% of the total. Dust sources accounted for 55% and 28% of PM_{10} and $PM_{2.5}$ emissions respectively. Agricultural sources accounted for 91% of NH_3 emissions. Major $PM_{2.5}$ species were OC, Ca, Si, PSO_4 and EC, accounting for 9.0%,

* Correspondence to C. Huang (huangc@saes.sh.cn)

7.0%, 6.4%, 4.6% and 4.3% of total $PM_{2.5}$ emissions respectively. The main species of NMVOCs were aromatic hydrocarbons, making up 25.3% of the total. Oxygenated volatile organic compounds (OVOCs) contributed 21.9% to the total NMVOC emissions. Toluene had the highest comprehensive contribution to ozone (O_3) and secondary organic aerosol (SOA) formation potentials, while other NMVOCs included 1,2,4-trimethylbenzene, m,p-xylene, propylene, ethene, o-xylene, ethylbenzene. Industrial process and solvent use sources were the main sources of O_3 and SOA formation potential, followed by motor vehicles. Among industrial sources, chemical manufacturing, rubber & plastic manufacturing, appliance manufacturing and textile made significant contributions. This emission inventory should provide scientific guidance for future control of air pollutants in the YRD region of China.

Key words: emission inventory; $PM_{2.5}$ species; NMVOC species; the Yangtze River Delta region; air pollutant emissions

1. Introduction

Air pollutant emissions from anthropogenic sources have attracted considerable attention due to their adverse impact on air quality (Monks et al., 2009), human health (Guan et al., 2016; Requia et al., 2018), and climate change (Fiore et al., 2012). Air pollutants include gaseous compounds such as sulfur dioxide (SO_2), nitrogen oxides (NO_x), carbon monoxide (CO), non-methane volatile organic compounds (NMVOCs), ammonia (NH_3), and particulate matter (PM) defined by diameters that are generally less than 10 μm, e.g. PM_{10} and $PM_{2.5}$ μm. NMVOCs are a large and diverse group of organic compounds, such as alkanes, alkenes, aromatic hydrocarbons and oxygenated volatile organic compounds (OVOCs). They are key precursors of ozone (O_3) and secondary organic aerosols (SOA). $PM_{2.5}$ are complex aggregates composed of e.g. sulfate (SO_4^{2-}), nitrate (NO_3^-), ammonium (NH_4^+), organic carbon (OC), elemental carbon (EC), and various elements. They can degrade atmospheric visibility and adversely affect human health (Qiao et al., 2014; Liang et al., 2016).

The emission inventory (EI) is an important tool for air pollution source

apportionment, air quality forecasting, and decision-making in air pollution control. In the last two decades, EI have improved on both global and regional scales. According to recent EI, anthropogenic emissions have shown increasing trends on a global scale (Janssens-Maenhout et al., 2015; Klimont et al., 2017; Crippa et al., 2018; Hoesly et al., 2018). China's air pollutant EI were at a higher level compared with the rest of the world due to increasing energy consumption, urbanization and vehicle population. However, China's emissions are undergoing dramatic changes, especially in key regions such as the Jing-Jin-Ji, Yangtze River Delta (YRD), and Pearl River Delta, which have seen the introduction of air pollution prevention and control measures in recent years (Cai et al., 2018; Zheng et al., 2018). Consequently, updating the national EI has become an important requirement.

The YRD region in eastern China, which includes areas of Jiangsu, Zhejiang, Anhui, and Shanghai, accounts for a significant proportion of China's population and gross domestic product (GDP). A rapidly growing economy and increased urbanization have resulted in the highest emission levels in China for this region. Data recently released by the Multi-resolution EI for China (MEIC, http://meicmodel.org/) showed that emissions of SO_2, NO_x, NMVOCs, $PM_{2.5}$, and NH_3, per unit area in the YRD region, were 2.3, 4.5, 5.2, 3.4, and 3.0 times, respectively, that of the national average. To understand the emission levels for the YRD region, Huang et al., (2011) established an EI for the core cities in 2007; Fu et al. (2013) updated the EI for Jiangsu, Zhejiang, and Shanghai in 2010 and refined the inventory of $PM_{2.5}$ and NMVOC speciation; in the last five years, only individual province (Zhou et al., 2017) and some sources were updated with the progress of method and data. Fan et al. (2016) established a high-resolved ship emission inventory for 2010 base on Automatic Identification System (AIS) data over the YRD region and East China Sea. Huang et al. (2018a) developed a non-road machinery emission inventory for 2014 based on local surveys in the cities of YRD. Zhang et al. (2020) further developed a "grid-based" (30 × 30 m) inventory of agricultural machinery with daily emissions for 2015 by combining satellite data, land

and soil information, and in-house investigation. Wang et al. (2018b) established an emission inventory of civil aviation for landing take-off (LTO) cycles for 2017. Yang and Zhao (2019) estimated air pollutant emissions from open biomass burning for 2005–2015 using three (traditional bottom-up, fire radiative power (FRP), and constraining) approaches. Zhao et al. (2020) developed a NH_3 emission inventory for 2014 based on dynamic emission factors (EFs) and activity data integrating the local information of soil, meteorology, and agricultural processes. These studies provided novel methods for emission estimation and expanded our understanding on the emissions over the YRD region. However, with the implementation of air pollution prevention and control measures, $PM_{2.5}$ pollution in the YRD region has improved significantly in recent years as the region's energy, industry, and vehicle structures have been modified accordingly (Zheng et al., 2016; Wang et al., 2017a; Zhang et al., 2017a). A comprehensive update of activity levels and sources in the YRD region could assist with accurate air quality simulations and emission reduction measures.

In addition to activity levels, speciation profiles of $PM_{2.5}$ and NMVOC emissions are required to improve the performance of chemical transport models (CTMs) that simulate O_3 mixing ratios and $PM_{2.5}$ concentrations. Source profiles from USEPA repository of organic gas and PM speciation profiles of air pollution sources (SPECIATE) were commonly used for source apportionment and create speciated EI for air quality modeling since the 1990s (USEPA, 2009; Simon et al., 2010). However, the emission characteristics of anthropogenic sources can vary considerably between different regions. Differences in fuel properties, operating conditions, raw materials, and after-treatment techniques can result in inconsistent speciation profiles for $PM_{2.5}$ and NMVOCs. A previous study indicated that use of speciation profiles from the SPECIATE database gave relatively poor model performance for trace elements at an urban site in Beijing, China (Ying et al., 2018). The emission estimates for individual NMVOC species varied by one to three orders of magnitude for some species when different sets of speciation profiles were used, which could result in significant

deviations in the outputs of O_3 and SOA simulations (Li et al., 2014; Zhao et al., 2017; Stroud et al., 2018; Wang et al., 2018c). Consequently, detailed and observation-based emissions of individual speciated $PM_{2.5}$ and NMVOCs have become essential for accurate CTM.

In this study, we updated an anthropogenic air pollutant EI for the 2017 YRD region using EFs and $PM_{2.5}$ and NMVOCs speciation profiles mainly derived from local measurements. The pollutants included: SO_2, NO_x, CO, NMVOCs, PM_{10}, $PM_{2.5}$, and NH_3; the NMVOC comprised 424 individual species such as alkanes, alkenes, aromatic hydrocarbons, haloalkanes and OVOCs; and 43 $PM_{2.5}$ species containing organic carbon (OC), elemental carbon (EC), ions, and elements. To obtain detailed emissions sources, the EI was refined into four categories, broadly based on fuel types, industrial sectors, equipment types, and emission levels, to give a total of 259 specific emission sources. Finally, the EI was validated using the Community Multiscale Air Quality (CMAQ) modeling system and observations from 2017 in the YRD region.

2. Materials and methods

2.1 Study domain

The YRD region in this study covers the three provinces of Jiangsu, Zhejiang, and Anhui, as well as Shanghai municipality. The region has a land area of approximately 350,400 km^2, accounting for 3.7% of the whole of China. The GDP for the region was 2,893 billion USD in 2017, i.e. ~24% of the total national GDP in that year and was growing at a rate of ~9.3% per year in the last decade (NBSC, 2018). Correspondingly, the region consumed 717.8 million ton coal equivalents of energy which was ~17% of the national total in 2017. Coal is the main energy type in the YRD, contributing ~60% of the total energy consumption (NBSC, 2018). The automobile population reached 40.9 million in 2017, accounting for 19.6% of the total in China. The region also has a high concentration of traditional industries, producing 13.9%, 11.3%, 9.0%, 18.2% and 19.1% of the total production of gasoline, diesel, coke, cement, and crude steel respectively in China in 2017 (NBSC, 2018). Figure 1 shows the domain of the YRD

region in this study. The coastal waters within the dashed line on the expanded image of the region are China's ship emission control areas. The ship emissions used in this study were a combination of emissions from this region and the inland waters of the YRD region.

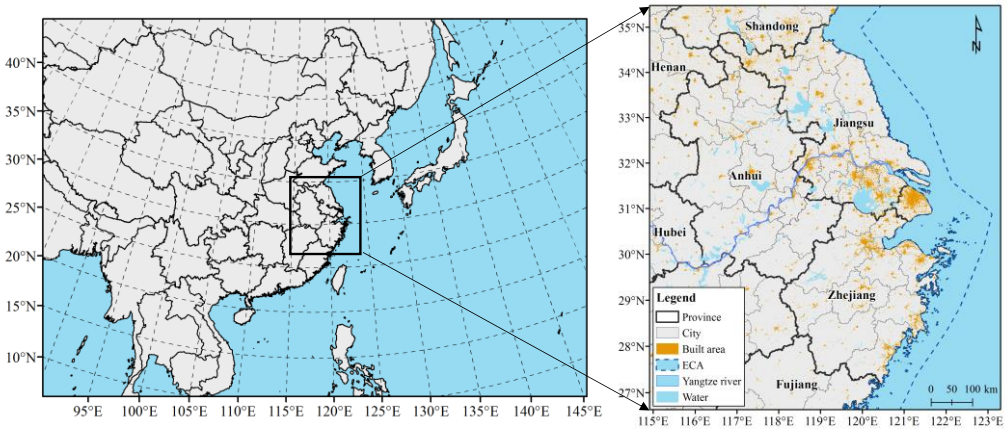

Figure 1. The domain of the YRD region in this study. Coastal waters within the dashed line on the expanded image represent ship emission control areas.

2.2 Sources classification

The EI was separated into four main categories. The first category was sub-divided into nine major sources including, stationary combustion, industrial process, industrial solvent-use, mobile, dust, oil storage and transportation, residential, waste treatment and disposal, and agricultural. The second category comprised 36 source types, mainly based on combustion facilities and the industrial, transportation, residential, and agriculture sectors. The third category comprised 127 sources classified mainly by fuel, product and material types. The fourth category included sources by combustion types, emission segments, and control levels. The detailed classification is shown in Table S1 of the supporting information.

2.3 Emission estimation methods

The emissions of SO_2, PM_{10}, and $PM_{2.5}$ from stationary combustion sources were calculated using the mass balance method according to Eq. (1) and (2). Other pollutant emissions were calculated using the EF method, given by Eq. (3).

$$E_{SO_2} = 2 \times S \times F \times C_s \times \left(1 - \eta_{SO_2}\right) \quad (1)$$

$$E_{PM} = A \times F \times C_A \times P_{ratio} \times (1 - \eta_{PM}) \quad (2)$$

$$E_{i,j} = AL_j \times EF_{i,j} \times \left(1 - \eta_{i,j}\right) \times 10^{-3} \quad (3)$$

Where: E_{SO2} and E_{PM} represent the emissions of SO_2 and PM_{10} or $PM_{2.5}$ (t); S and A represent fuel sulfur content and ash in fuel (%); F is the fuel consumption (t); Cs and C_A are the conversion efficiencies from sulfur and ash to SO_2 and PM (%); P_{ratio} is the mass percentage of PM_{10} or $PM_{2.5}$ in total PM; η_{SO2} and η_{PM} represent the removal efficiency of SO_2 and PM_{10} or $PM_{2.5}$; $E_{i,j}$ represents the emissions of pollutant i from source j (t); AL_j is the activity data of source j, such as fuel consumption, product output, and raw material consumption; $EF_{i,j}$ is the EF of pollutant i from source j (kg per activity data); $H_{i,j}$ is the removal efficiency of pollutant i from source j.

Emissions from the industrial process sources were calculated using the EF method shown in Eq. (3). For large point sources, we established a segment-based emission estimation method based on local surveys. For example, we subdivided the ferrous metal manufacturing industry into raw material yard, iron making (including sintering, pelletizing, and blast furnace), steel making (including converter and electric furnace), casing steel, rolling steel, and ferroalloy production. The petroleum refining industry was subdivided into eight segments including process devices, equipment leak, storage tank, bulk loading, flare, wastewater treatment, cooling tower, and petrochemical furnace. The activity data and EFs of each segment were both derived from on-site surveys and measurements. Emissions from industrial solvent-use sources were calculated using the mass balance method based on the consumption and NMVOC content of solvents, such as paints, coatings, inks, adhesives, thinners, etc. Small amounts of NMVOC remaining in products, wastewater and waste were not considered in this calculation. The solvent consumption and their VOC content of large point sources were mainly from field surveys and then extended to similar industries and solvent varieties.

For motor vehicles, the International Vehicle Emission (IVE) model was used to

calculate the emissions. However, the EFs and activity data for driving conditions, fleet composition, vehicle mileage traveled (VMT), and meteorological parameters in the model were restricted to real-world measurements and surveys. Non-road machinery emissions were estimated from the NONROAD model (USEPA, 2010), which was based on fuel consumption and fuel-based EFs. Fuel consumption was calculated from the population, working hours and fuel consumption rate per hour derived from local survey in typical cities like Shanghai and Hangzhou. The method was introduced in our previous study (Huang et al., 2018a). Limited by the data source, we haven't achieved a daily-resolved emission estimation of agricultural machinery introduced by Zhang et al. (2020), which may cause higher uncertainty on its total amount and temporal and spatial distribution. Ship emissions were estimated according to the method of Fan et al. (2016) using an approach based on the AIS data. The civil aviation aircraft source included emissions defined by the International Civil Aviation Organization (ICAO) for LTO cycles, which included approach, taxi, take-off, and climb. SO_2 emission from the civil aviation aircraft source was estimated using the mass balance method. The sulfur content in aviation fuel of 0.068% was the default value provided in a previous study (Wayson et al., 2009). NO_x, CO, and NMVOC emissions were estimated using the EF method as the product of fuel consumption rate and EFs. PM emission was calculated using the first-order approximation (FOA3.0) method (Wayson et al., 2009). The rated thrust and working hours of the aircraft in each LTO cycle were referenced from the parameters recommended by ICAO. The climbing mode specified by ICAO referred an altitude of ~1 km from the end of take-off to the top of the atmospheric boundary layer. However, since the height of boundary layer was dependent on meteorological conditions, The Weather Research and Forecast (WRF) Model (version 3.9.1) was used to simulate the boundary layer height and correct the duration of the climbing mode. A detailed description of the method used for aviation emission estimation is provided in our previous study (Wang et al., 2018b).

Emissions from other sources (dust, oil storage and transportation, residential,

waste treatment and disposal, and agricultural) were all calculated using the EF method.

The emission estimation method of this study has been improved on the basis of our previous study (the latest version was for 2014) (Li et al., 2019; Ni et al., 2020). Table 1 shows the differences between the methods and data sources of this study and the previous. First, the source category has been refined from the third-level 135 categories to the fourth-level 2812 categories. Among them, large point sources such as iron & steel and petroleum refining sectors were further subdivided into different emission segments. Secondly, in addition to the environmental statistics data, the activity data has been refined through local investigations on the removal technologies and efficiencies, operating hours, and working conditions of industrial and mobile sources including motor vehicles and non-road machinery; emissions from ships and aircrafts, which were not considered in our previous study, were estimated based on dynamic activity data like AIS provided by local department. In terms of the EFs, most of them were corrected based on local measurements.

Table 1. Comparison of the methods and data sources in this study with our previous study.

Methods/Data sources	This study	Our previous study
Source classification	2812 source categories, subdivided into four levels, detailed to emission segments for large point sources	135 source categories, subdivided into three levels
Activity data		
Stationary combustion sources	Based on environmental statistics	Based on environmental statistics
Industrial process sources	Based on environmental statistics and local investigation on removal technologies and efficiencies	Based on environmental statistics
Industrial solvent-use sources	Based on environmental statistics and local investigation on solvent types and consumption	Based on environmental statistics
Motor vehicles	Based on city statistics and local activity surveys	Based on city statistics and local activity surveys
Non-road machinery	Based on city statistics and local activity surveys	Not considered
Ships	Based on AIS data	Not considered
Aviation aircraft	Based on LTO cycles from department surveys	Not considered

Dust sources	Estimated based on city statistics	Estimated based on city statistics
Oil storage and transportation sources	Based on city statistics	Based on city statistics
Residential sources	Based on city statistics	Based on city statistics
Waste treatment and disposal sources	Based on city statistics	Based on city statistics
Livestock and poultry breeding	Based on city statistics	Based on city statistics
N-fertilizer application	Based on city statistics	Based on city statistics
Biomass burning	Estimated based on city statistics	Estimated based on city statistics
EFs		
Stationary combustion sources	Based on literature surveys	Based on literature surveys
Industrial process sources	Updated the EFs for major segments of iron & steel and petroleum refining sectors based on local measurements	Based on literature surveys
Industrial solvent-use sources	Estimated by solvent contents of different solvent types from local investigations	Based on literature surveys
Motor vehicles	IVE model corrected by local measurements	IVE model
Non-road machinery	NONROAD model corrected by local measurements	Not considered
Ships	Based on local measurements	Not considered
Aviation aircraft	Recommended by ICAO	Not considered
Dust sources	Based on literature surveys	Based on literature surveys
Oil storage and transportation sources	Estimated based on local investigations	Based on literature surveys
Residential sources	Based on local investigations and measurements	Based on literature surveys
Waste treatment and disposal sources	Based on literature surveys	Based on literature surveys
Livestock and poultry breeding	Based on local measurements	Based on literature surveys
N-fertilizer application	Based on local measurements	Based on literature surveys
Biomass burning	Based on local measurements	Based on literature surveys

2.4 Activity data sources

Activity data related to the industrial sources (e.g. stationary combustion sources, industrial process and solvent-use sources) were mainly from the 2017 Environmental Statistics Database, which contained information on fuel consumption, product output, raw material consumption, and removal technology and efficiencies. There were ~30,000 major point sources for the YRD region in the database. However, the database didn't include all the information like the technologies of NMVOC removal and their efficiencies, especially for the median and small-size factories. To obtain more detailed

information, we have conducted more on-site investigations on the removal technologies and efficiencies of industrial sources in typical cities including Shanghai, Hangzhou, Suzhou, etc. According to the investigations, we classified the proportions of removal technologies and efficiencies to different industrial sectors and then extended them to the entire region. As environmental statistics do not include all industrial sources, we derived an area source using the difference between the total fuel consumption and product output in the statistical yearbook and the sum of environmental statistics for each city. To improve the accuracy of mobile source emissions, several local activity surveys (e.g. population, vehicle or machine type, fuel type, and emission standard) were conducted for motor vehicles, non-road machinery, and civil aviation aircraft. The activity data of ships was obtained from the AIS data for the East China Sea in 2017. The activity data of area sources were derived from the statistical yearbooks of cities in the YRD region. Sources of activity data not recorded in the statistical yearbooks (e.g. the number of construction sites, civil solvent usage, catering, biomass burning) were estimated from statistical data, such as population, building area, and crop yields. The biomass burning emissions in this study only included the emissions from household biomass-fueled stoves. Their activity data was estimated based on the crop yields and grain straw ratios combined with the proportions of household burning in each city. The crop yields were obtained from the statistical yearbooks; the grain straw ratios and the proportions of household burning were derived from the surveys from agricultural department. In 2017, the average household burning ratio of various types of straw was about 12% (3%–16%), 3% in developed cities such as Shanghai; the highest ratios (16%) were in the cities of Anhui Province; and the ratios in other cities were about 12%.Table S2 in the support information summarizes the emission estimation methods, activity data sources and their data reliability.

2.5 Determination of EFs

The EFs of each specific emission source were determined by local measurements (or surveys) in the YRD region, domestic EI guidebook of China (MEP, 2014), and

those given in USEPA Compilation of Air Pollutant Emissions Factors (AP-42; USEPA, 2002) and Joint European Monitoring and Evaluation Programme (EMP)/European Environment Agency (EEA) datasets (EEA, 2013) respectively. To minimize uncertainty in the EI, this study localized the EFs from 80 source categories. This included the majority of anthropogenic emission sources, such as coal-fired power plants and boilers (Yao et al., 2009; Zhao et al., 2010; Wang et al., 2011; Lou, 2014; Sun, 2015; Xu et al., 2018), petroleum refining and ferrous metal manufacturing (Guo et al., 2017), gasoline and diesel vehicles (Huang et al., 2016; Huang et al., 2017; Huang et al., 2018b; Huang et al., 2018c), non-road machinery (Fu et al., 2012; Fu et al., 2013; Ge et al., 2013; Qu et al., 2015; Li et al., 2016), emissions from cooking (Wang et al., 2018a; Gao et al., 2019), livestock and poultry breeding (Chen, 2017; Zhou, 2019), N-fertilizer application (Chen et al., 2017; Xia et al., 2018), and biomass burning (Tang et al., 2014). NMVOC EFs for some evaporation loss sources, such as industrial and residential solvent-use, oil storage, and transportation, were estimated from the results of field surveys of typical sources in the YRD region. For sources that could not be measured or investigated, the EFs were obtained in the following order of preference: EI guidebook of China (MEP, 2014)>USEPA AP-42 (USEPA, 2002)>EMEP/EEA datasets (EEA, 2013). The EFs for each source and their references are provided in Table S1 of the supporting information.

2.6 $PM_{2.5}$ and NMVOC speciation

$PM_{2.5}$ and NMVOC emissions were converted into profiles of individual species to simulate $PM_{2.5}$ chemical components and O_3 mixing ratios in the atmosphere. The profile for $PM_{2.5}$ comprised 43 chemical species, including OC, EC, particulate sulfate (PSO_4), nitrate (PNO_3), and ammonium (PNH_4) and 36 elemental components such as Na, Mg, K, Ca, Al, and Si, etc. Additional species such as particulate H_2O, noncarbon organic matter, metal bound oxygen, and other unspeciated $PM_{2.5}$ were calculated according to the method of Reff et al. (2009). The profile for NMVOC included 96 alkanes, 45 alkenes and alkynes, 44 aromatic hydrocarbons, 164 OVOCs, 43

haloalkanes, and 32 other organic compounds.

The method used to determine the $PM_{2.5}$ and NMVOC source profiles followed that used for the EFs and data was preferentially selected as follows: local measurements>measurements from previous domestic studies>USEPA SPECIATE 4.4 database (Hsu et al., 2014). To improve the representativeness of source profiles in the inventory, the $PM_{2.5}$ chemical compositions from 34 sources and the NMVOC chemical compositions from 64 sources were localized according to the measurements in the YRD region. Source categories used for the localized $PM_{2.5}$ profiles included power plants, coal-fired boilers, ferrous metal manufacturing, gasoline and diesel vehicles, non-road machinery, ships, catering, and biomass burning (Zheng et al., 2013; Tang et al., 2014; Huang et al., 2016; Xu et al., 2018). The source categories used for the localized NMVOC profiles included coal combustion, gasoline and diesel vehicles, ships, catering, biomass burning, and the majority of industrial process and solvent-use sources, such as petroleum refining, coke production, chemical manufacturing, textile, furniture manufacturing, package and printing, auto manufacturing, shipbuilding, and architectural coating (Wang et al., 2014a; Wang et al., 2014b; Wang et al., 2016; Wang et al., 2017b; Wang et al., 2017c; Huang et al., 2018d; Gao et al., 2019). Detailed information concerning references, samples, and sampling and analytical methods for the sources are given in Table S3. For those species which could not be determined by analytical methods, the mass fraction data was supplemented with that obtained from the SPECIATE database. Figure 2 shows the $PM_{2.5}$ and NMVOC speciation profiles for the major emission sources in the YRD region.

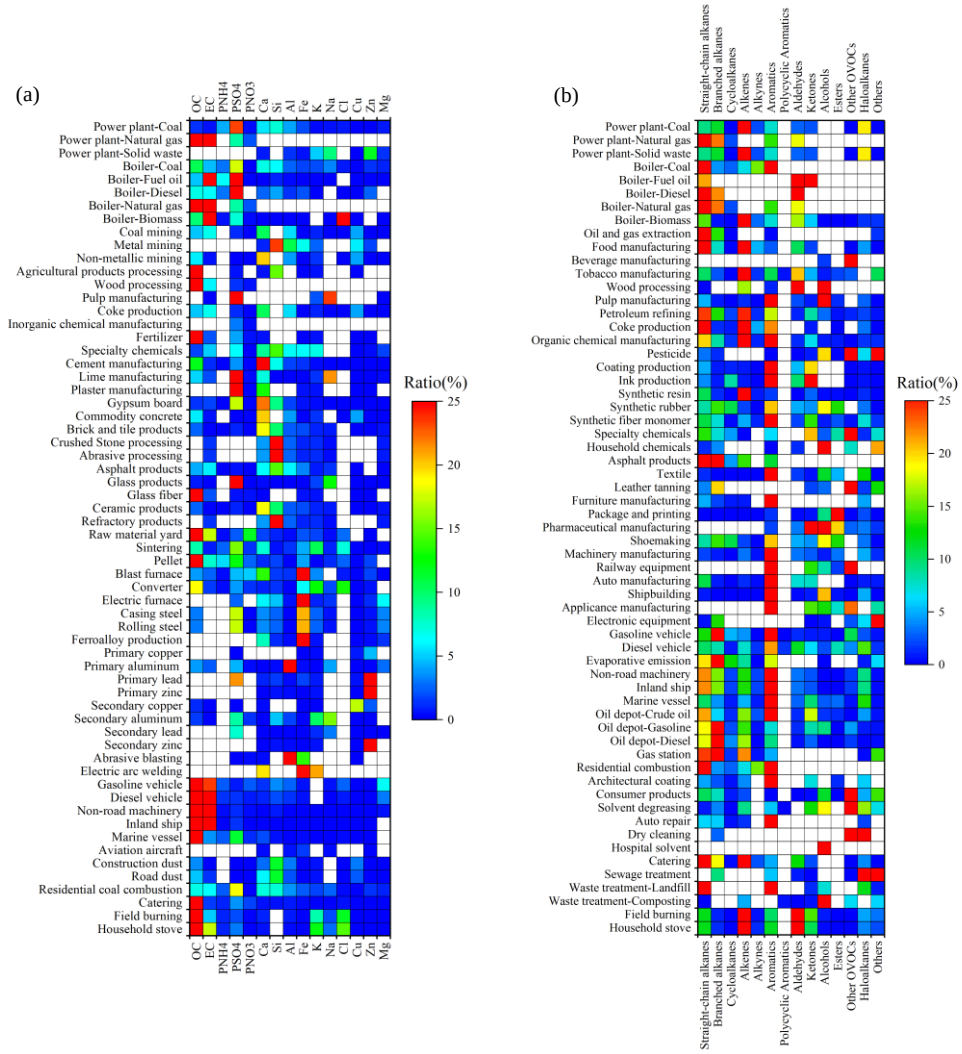

Figure 2. Speciation profiles for the major emission sources: (a) $PM_{2.5}$; and (b) NMVOCs.

2.7 Spatial distributions

Emissions from industrial sources, e.g. power plants, boilers, industrial process and solvent-use sources, were allocated from the Environmental Statistics Database based on their geographical coordinates. Vehicle emissions were calculated from the mileage distributions of various vehicle categories on different types of road. The composition of traffic flow on different types of road was obtained from previous surveys in Shanghai and Hangzhou (Huang et al., 2015; Yang et al., 2017). The approach of spatial allocation for road dust was consistent with that used for vehicle emissions. The spatial distribution of emissions from non-road machinery varied depending on the type of machinery. The emissions from construction and agricultural machinery were allocated according to urban and farmland areas given in the 2015 land

use data released by European Space Agency (ESA) (https://www.esa-landcover-cci.org/). Emissions from port and factory machinery, and airport ground handling equipment were assigned according to their geographical coordinates. Emissions from residential sources were assigned from population distribution data with a 1 km resolution. Emissions from agricultural sources were allocated from farmland areas in the land use data (ibid.).

2.8 Uncertainty analysis

Uncertainty was mainly derived from the activity data and EFs. The coefficients of variation of the activity data and EFs for each source were classified into seven grades in the range of 2%–100% using expert judgment. The coefficient of variation for the activity data was determined according to the data source. Environmental statistical data with specific source information was assigned the lowest coefficient of uncertainty (2%), while activity data estimated from the statistical yearbooks, such as biomass burning, was assigned the highest uncertainty value (98%). The coefficients of uncertainty for other activity data sources were assigned to be 18%, 34%, 50%, 66%, and 82% in turn. The principle for assignments of the coefficients of variation for EFs was the same as the activity level. EFs derived from local measurements in the YRD region with large samples were assigned the lower coefficients of uncertainty (18%), while those from USEPA or EMEP/EEA datasets were assigned higher coefficients (98%). Then the uncertainty of each pollutant from each emission source can be combined by Eq. (3–5). A detailed description of the analytical methods used can be found in our previous study (Huang et al., 2011).

$$CV = \frac{U}{E} = 1.96 \times \sqrt{(1 + C_a^2) \times \left(1 + C_f^2\right) - 1} \quad (3)$$

$$U_j = \sqrt{\sum_k U_{j,k}^2} \quad (4)$$

$$U = \sqrt{\sum_{j} U_j^2} \quad (5)$$

where, CV is the coefficient of variation of the emission rate, E is the emission rate, U is the uncertainty of the emission source, C_a is the uncertainty of activity data, C_f is the uncertainty of EF, j and k represent for pollutant and emission source, respectively.

2.9 Model configurations

To verify the reliability of the EI, we used CMAQ (version 5.3) to simulate the concentrations of SO_2, NO_2, $PM_{2.5}$, PM_{10}, O_3, and CO in the YRD region for January and July 2017, and compared these with the observation data for each city in the region. The meteorological field for the CMAQ model was obtained from the WRF (version 3). The EI developed in this study was then used to produce an emission system for the YRD region while emissions beyond the YRD were obtained from the MEIC 2016. The anthropogenic data was then combined with biogenic data obtained from the Model for Emissions of Gases and Aerosol from Nature modelling system (version 2.10) as the final input for the EI of the model. Figure S1 and Table S6 show the domain and settings for the model system. Detailed information is provided in Section 6 of the Supporting information.

2.10 Estimation of O_3 and SOA formation potentials

To characterize the regional O_3 and SOA formation contributions of different NMVOC species and their sources, we used the O_3 formation potential (OFP) and SOA formation potential (SOAP) methods of estimation. OFP and SOAP were obtained from the sum of the individual NMVOC species emissions multiplied by the maximum incremental reactivity (MIR) and SOA yield, respectively. MIR and SOA yield for individual NMVOC species were obtained from previous studies (Carter, 1994; Wu and Xie, 2017). The estimation methods were shown in Eq. (6) and (7).

$$OFP_i = \sum_{j=1} E_{i,j} \times MIR_j \quad (6)$$

$$SOAP_i = \sum_{j=1} E_{i,j} \times Y_j \quad (7)$$

where, OFP_i and $SOAP_i$ are the ozone formation potential and SOA formation potential of source i, respectively, $E_{i,j}$ is the VOC emission of species i, MIR_j is the maximum increment reactivity for the jth chemical species, Y_j is the SOA yield for the jth chemical species.

3. Results and discussion

3.1 Emission and source contributions

3.1.1 Emissions and comparisons with previous studies

The total emissions of SO_2, NO_x, CO, NMVOCs, PM_{10}, $PM_{2.5}$, and NH_3 in the YRD region for the year of 2017 were 1,552, 3,235, 38,507, 4,875, 3,770, 1,597 and 2,467 Gg, respectively. Excluding ship emissions, the air pollutant emissions were 1,437, 2,936, 38,486, 4,867, 3,754, 1,583 and 2,467 Gg, respectively. Detailed information of air pollutant emissions for each city is shown in Table S1 of the supporting information.

Table 2 shows the estimated emissions for the YRD region and their comparison with previous studies. SO_2 emissions were close to that from the MEIC in 2016 and much lower than those reported in 2015. Emission reductions from coal-fired facilities, including power plants and boilers, could be the main reason for the significant decline in SO_2 emissions (Zheng et al., 2018). NO_x emissions were generally lower than the results from previous studies. Some modeling and satellite studies verified that the NO_x emissions in previous studies were overestimated, partly due to improvements in NO_x control measures for the power sector which were not considered at that time (Zhao et al., 2018; Sha et al., 2019). The NO_x EFs for coal-fired power plants and boilers in this study were derived from local measurements which were generally lower than those in previous studies, so the NO_x emissions from the power sector were 47% lower than those from the MEIC. CO emissions were higher than the MEIC results but similar to those reported by Sun et al. (2018a). NMVOC emissions for key sources in this study

were individually estimated using the "bottom-up" method, so the estimates were lower than those using the "top-down" approach. In addition, most of the EFs selected in this study were detailed into different process segments, which were generally lower than the comprehensive EFs used for whole industrial sectors in previous studies. Since dust sources were not included in the MEIC inventory, PM_{10} and $PM_{2.5}$ emissions estimated in this study were 1.7 and 0.5 times higher, respectively. A previous study also showed that NH_3 emissions in China were underestimated, mainly due the application of lower emission rates from fertilizer applications and livestock and the omission of other sources (Zhang et al., 2017). Therefore, we used local measured NH_3 EFs for fertilizer application and some of the livestock breeding sources in the YRD region. NH_3 emissions from the transportation sector were also higher (by a factor of 2.8) than those from the MEIC due to the localized NH_3 EFs from light-duty gasoline vehicles (Huang et al., 2018) used in this study. In addition, NH_3 slip from selective catalyst reduction devices in the power sector (not included in previous studies) was also considered in this study.

Compared with our previous inventory for 2014 (Li et al., 2019; Ni et al., 2020), SO_2, NO_x, PM_{10}, and $PM_{2.5}$ emissions in the YRD region have decreased by 47%, 15%, 20%, and 24%, respectively, which were consistent with the trends of regional air quality improvement (SO_2 44 %; NO_2 5%; PM_{10} 22%; $PM_{2.5}$ 27%). However, it should be noted that the approach of emission estimation in this study has made a number of localized corrections in terms of emission factors and activity data. For example, CO, NMVOC, and NH_3 emissions have increased significantly compared to 2014, which mainly because more point sources were included in this study and more localized EFs, which were generally higher than those in previous studies, were applied to estimate NOx, CO, NMVOC, and NH_3 emissions from solvent-use, motor vehicle, non-road machinery, and agricultural sources. Next, it is necessary to estimate the emission inventories by the same approach for different years to evaluate the changes in air pollutant emissions in recent years.

428 **Table 2.** Air pollutant emissions in the YRD region and their comparison with other studies.

Regions	Data source	Base year	Annual air pollutant emissions (Gg/year)						
			SO_2	NO_x	CO	NMVOCs	PM_{10}	$PM_{2.5}$	NH_3
YRD	This study	2017	1,437	2,936	38,486	4,867	3,754	1,583	2,467
	MEIC	2016	1,136	3,753	19,560	5,527	1,374	1,025	1,153
	Simayi et al., 2019	2016				4,984			
	Sun et al., 2018a	2015	3,050	4,160	30,210	5,490			
	Zhang et al., 2017b	2015							1,632
	Our previous study	2014	2,737	3,457	33,118	4,069	4,681	2,085	1,582
	Wu et al., 2018	2013				6,198			
Shanghai	This study	2017	57	225	1,393	418	124	56	54
	MEIC	2016	168	345	1,192	683	69	51	25
	Simayi et al., 2019	2016				728			
	Sun et al., 2018a	2015	550	470	2250	580			
	Zhang et al., 2017b	2015							50
	Our previous study	2014	100	256	1,699	391	197	93	73
	Wu et al., 2018	2013				838			
	Fu et al., 2013	2010	260	453		422	86	59	65
Jiangsu	This study	2017	619	1,165	17,309	2,056	1,440	577	1,093
	MEIC	2016	468	1,586	8,191	2,128	516	388	532
	Simayi et al., 2019	2016				2,024			
	Sun et al., 2018a	2015	1,230	1,700	13,780	2,000			
	Zhang et al., 2017b	2015							703
	Our previous study	2014	1,002	1,315	12,667	1,560	1,761	779	544
	Wu et al., 2018	2013				2,240			
	Zhou et al., 2017	2012	1,142	1,642	7,680	1,747	1,394	941	1,100
	Fu et al., 2013	2010	1,126	1,257		1,759	619	401	976
Zhejiang	This study	2017	339	676	7,036	1,484	775	308	363
	MEIC	2016	280	867	3,779	1,671	219	151	159
	Simayi et al., 2019	2016				1,624			
	Sun et al., 2018a	2015	730	980	5,110	1,810			
	Zhang et al., 2017b	2015							257
	Our previous study	2014	646	903	9,372	1,346	1,199	508	374
	Wu et al., 2018	2013				2,214			
	Fu et al., 2013	2010	762	1,067		1,641	301	184	398
Anhui	This study	2017	422	869	12,748	910	1,415	642	957
	MEIC	2016	221	954	6,398	1,045	570	435	437
	Simayi et al., 2019	2016				608			
	Sun et al., 2018a	2015	540	1,010	9,070	1,100			
	Sun et al., 2018b	2015	434	688				323	422
	Zhang et al., 2017b	2015							622

Our previous study	2014	725	983	9,380	772	1,524	706	592
Wu et al., 2018	2013				906			

3.1.2 Source contributions

Figure 3 shows the emission contributions of the major air pollutants in the YRD region from the main category sources (a), industrial sector sources (b), and mobile sources (c). Further detailed information of emissions from each source is provided in Table S5. SO_2 and CO emissions were mainly from boilers, accounting for 49% and 73% of the total emissions, respectively. Notably, emission contributions from power plants were significantly lower than those from previous inventories (MEIC, http://meicmodel.org/; Zhou et al., 2017), resulting mainly from the implementation of stringent emission reduction measures in recent years (Wu et al., 2019; Zhang et al., 2019).

Mobile sources accounted for the majority (57%) of NO_x emissions in the YRD region which was generally higher contributions given in the MEIC and other EI (Zhou et al., 2017; Sun et al., 2018a). Emission control measures for power plants had demonstrably reduced NO_x emissions. In addition, ship emissions, which had not been included in previous studies, accounted for 16% of NO_x emissions from mobile sources in the YRD region (see Figure 3(c), 'Marine'). Furthermore, NO_x EFs for gasoline and diesel vehicles used in this study, derived from local measurements, were generally higher than those given by MEP (2014). Some real-world measurements based on portable emission measurement systems, on-road chasing, and tunnel experiments also indicated that the NO_x emissions from vehicles in China were higher than expected, probably due to deficiencies in the type-approval protocols and emission controls (Wu et al., 2012; Huang et al., 2017; Song et al., 2018; Wen et al., 2019).

Industrial sources accounted for the majority of total NMVOC emissions (61%), of which industrial process and solvent-use sources contributed 34% and 27%, respectively. Mobile and residential sources contributed 20% and 10%, respectively. Dust sources were the main contributors to PM_{10} (55%) and $PM_{2.5}$ (28%) emissions.

Agricultural sources accounted for 91% of NH_3 emissions with minor contributions from residential (3%) and mobile (1%) sources. Although NH_3 EFs from vehicles were considered in this study, their emissions were significantly lower than those from agricultural sources. However, vehicle emissions were mainly concentrated in urban areas where their contribution to NH_3 emissions would be considerable.

Industrial emissions of SO_2 and CO were mainly from the five major sectors of petroleum refining, coking, chemical manufacturing, non-metallic mineral manufacturing, and ferrous metal manufacturing. Non-metallic mineral manufacturing and ferrous metal manufacturing dominated the industrial NO_x, PM_{10}, and $PM_{2.5}$ emissions. The top five industrial sector sources of NMVOCs emissions in the YRD region were chemical manufacturing, furniture and wood manufacturing, appliance manufacturing, rubber and plastic manufacturing, and non-metallic mineral manufacturing. These accounted for 27%, 12%, 9%, 9%, and 6% of the total NMVOC emissions respectively. Chemical manufacturing contributed to the majority of industrial NH_3 emissions in the YRD region.

The ports and harbors of the YRD region are collectively the largest group in the world and, as expected, emissions from the transportation of ships and heavy-duty trucks dominated the mobile source emissions. Ships accounted for 94%, 16%, 12%, and 12% of mobile source SO_2, NO_x, PM_{10}, and $PM_{2.5}$ emissions, respectively while heavy-duty trucks contributed 31%, 37%, and 36% to mobile source NO_x, PM_{10}, and $PM_{2.5}$ emissions respectively. Light-duty vehicles contributed significantly to CO, NMVOCs, and NH_3 emissions, accounting for 61%, 46%, and 90%, respectively. Non-road machinery accounted for 27%, 18%, 12%, 21%, and 22% of NO_x, CO, NMVOCs, PM_{10}, and $PM_{2.5}$ emissions from mobile sources respectively. Construction and agriculture machinery were also major contributors.

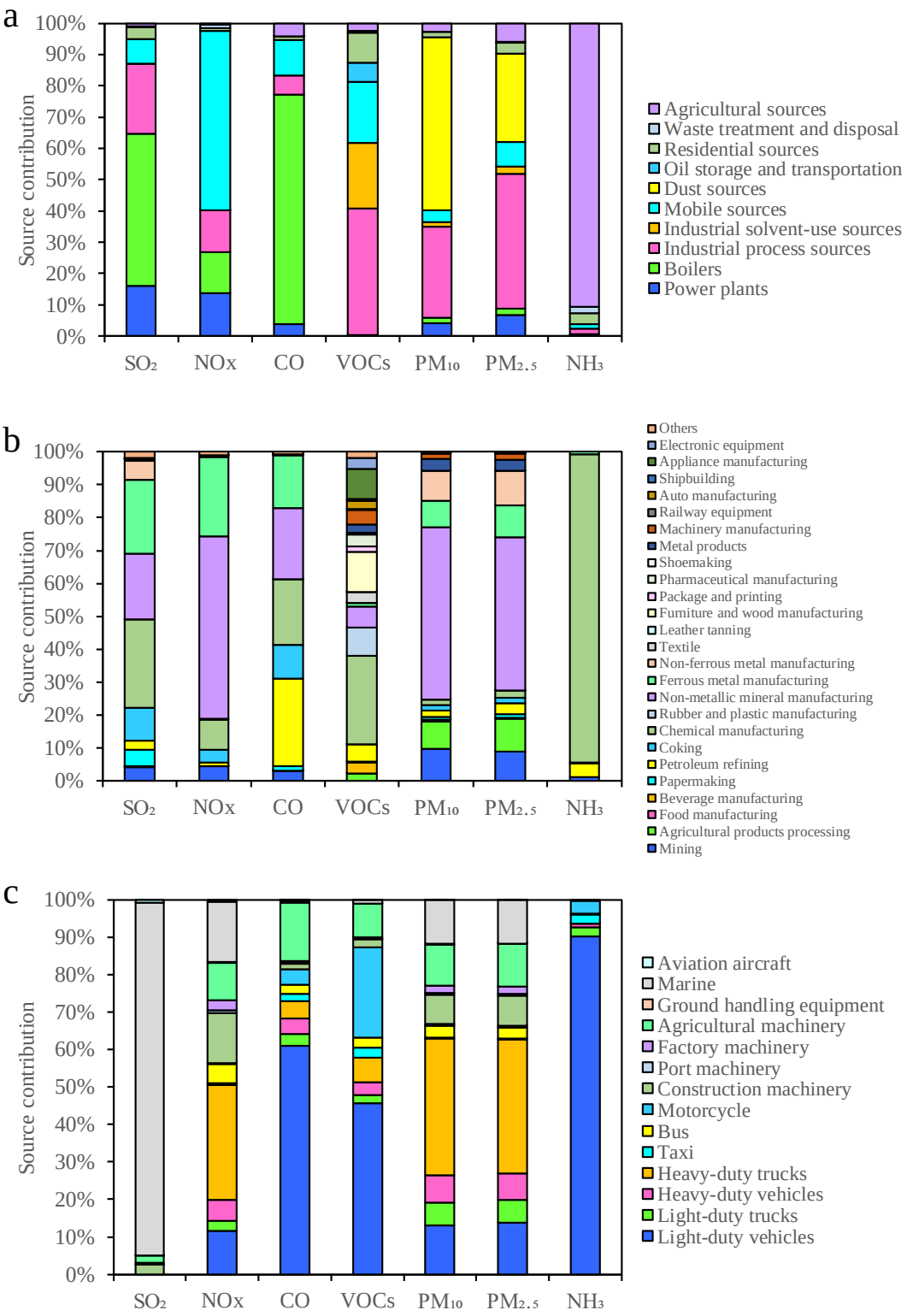

Figure 3. Emission contributions of major air pollutants in the YRD region from: (a) Major category sources; (b) industrial sector sources; (c) mobile sources.

3.1.3 Spatial distribution

Figure 4 shows the spatial distribution of SO_2, NO_x, CO, NMVOCs, $PM_{2.5}$, and

NH_3 emissions in the YRD region. SO_2 emissions were mainly concentrated in the high-density shipping regions of the Yangtze River and East China Sea estuary. SO_2 emissions from power plants and boilers along the Yangtze River and in cities of northern Anhui and Jiangsu provinces were also significant in these regions. The spatial distribution of NO_x and NMVOCs was similar and mainly concentrated along the Yangtze River and Hangzhou Bay where industry and logistics were most developed. CO and $PM_{2.5}$ emissions were mainly concentrated in the urban areas of cities due to intensive road traffic and construction work. NH_3 emissions were relatively high in northern Anhui and Jiangsu provinces, resulting mainly from their developed agriculture. Large cities such as Shanghai presented higher NH_3 emission intensities, largely due to contributions from residential and mobile sources.

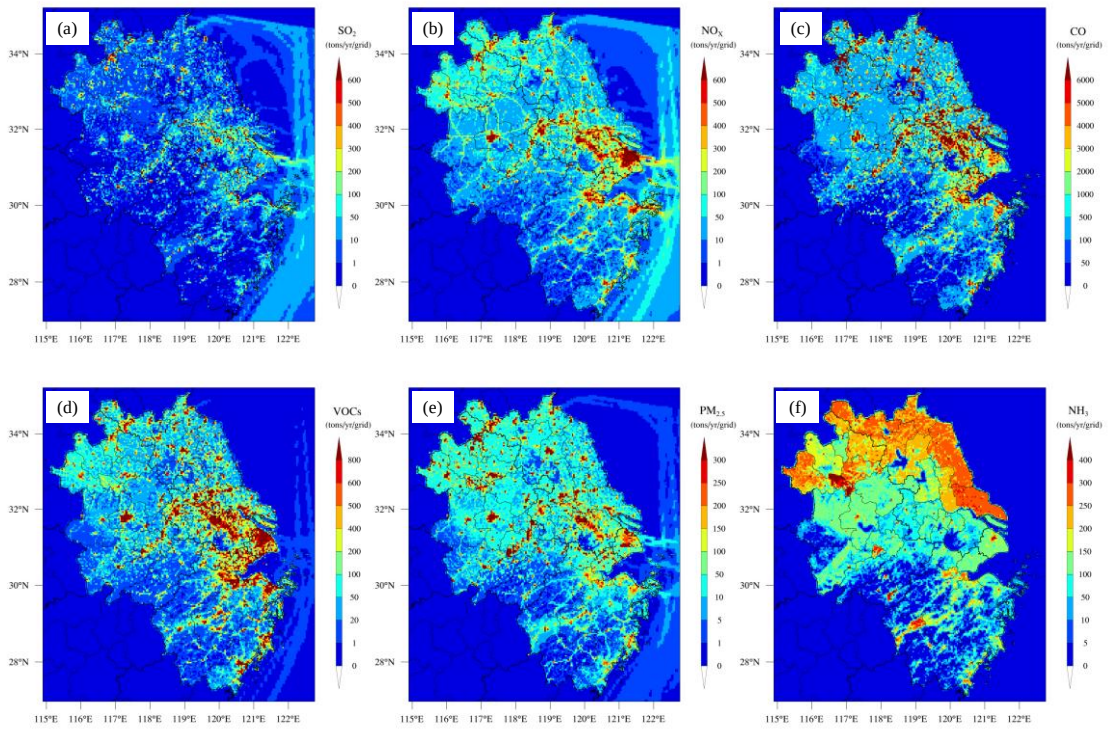

Figure 4. Spatial distribution of major air pollutant emissions in the YRD region: (a)~(f) Represent SO_2, NO_x, CO, NMVOCs, $PM_{2.5}$, and NH_3 respectively.

Figure 5 shows the spatial distribution of NO_x and NMVOCs from the major industrial sectors in the YRD region. There were large differences in the spatial distribution of the different industrial sectors. Key sources of NO_x emissions, shown in Figure 5(a)-(d), included: Power plants mainly distributed along the Yangtze River and

Hangzhou Bay and the northern part of the YRD region; iron and steel manufacturing concentrated along the Yangtze River; and cement and brick manufacturing mainly distributed in the western and northern regions of the YRD. Compared with NOx emissions, the key sources of NMVOC (Figure 5(e) -(l)) were mainly concentrated in the central and eastern regions of the YRD. These included the regions of Shanghai, Suzhou, Wuxi, Changzhou, Nanjing, Hangzhou, Ningbo, Jiaxing, and Shaoxing, which also had the highest NO_x emission intensities in the YRD region. High levels of NO_x and NMVOC were key factors responsible for harmful pollution by secondary PM and O_3 in this region (Li et al., 2018; Li et al., 2019).

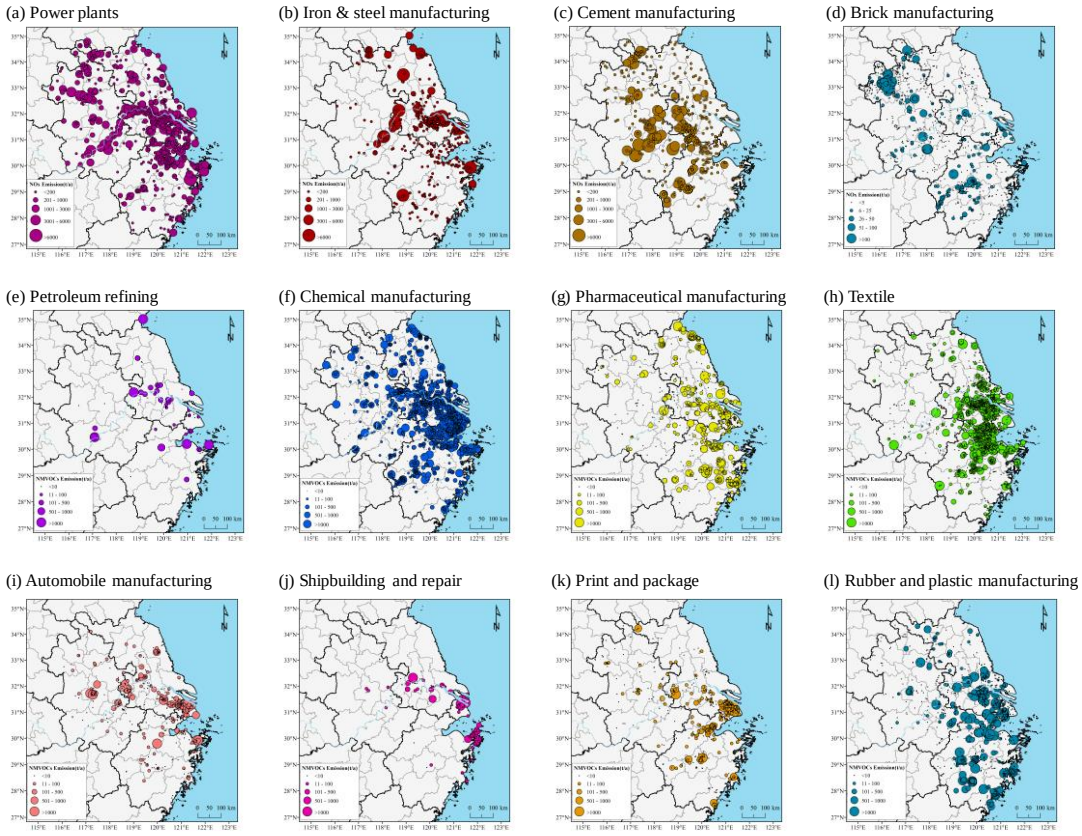

Figure 5. Spatial distribution of the major NO_x and NMVOC emission sources in the YRD region.

Previous studies have shown that the unit-based bottom-up approach based on local activity data can improve the spatial distribution of emission inventories (Zhao et al., 2015; Zheng et al., 2017; Zhao et al., 2018; Zheng et al., 2019). The spatial distribution of major air pollutants obtained in this study is consistent to other unit-based inventories based on local surveys. For example, the distribution of NMVOC

emissions is consistent with that obtained from the on-site surveys in Jiangsu Province (Zhao et al., 2017); the distribution of NH_3 emissions is also consistent with the results using dynamic emission factors and localized information (Zhao et al., 2020). Compared with the national-scale inventory like the MEIC, this study has improved the distribution along the Yangtze River and Hangzhou Bay where large point sources were denser, and it also reduced the misjudgment of NO_x and NMVOC emission hotspots in the northern and southern areas, as shown in Figure S1. The distribution of NH_3 emissions was also improved in the northern areas of the region and in the city centers with more localized EFs of mobile and agriculture sources.

3.1.4 Uncertainty assessment

The EI was compiled using the bottom-up approach based on local EFs and activity data from the region. The activity data for industrial sources, including fuel consumption, sulfur content, ash content, raw material used, and control efficiency, were collected from the Environmental Statistics Database. EFs from some key sources, such as coal-fired power plants and boilers, iron and steel manufacturing, gasoline and diesel vehicles, non-road machinery, catering, and agricultural sources, were modified based on the local measurements. These measured helped to reduce the uncertainty of the emission estimates. Table 3 shows the uncertainties of major sources at the 95% confidence interval in this EI. The average uncertainties of emissions from the YRD region were estimated as -29 to 36% for SO_2, -28 to 33% for NO_x, -42 to 75% for CO, -44 to 68% for NMVOCs, -36 to 62% for PM_{10}, -30 to 46% for $PM_{2.5}$, and -58 to 117% for NH_3. The overall uncertainties were lower compared with our previous EI for the YRD region (Huang et al., 2011).

The uncertainty assessment indicated that emissions from stationary combustion sources, such as power plants and boilers, were more reliable, because the estimates were based on detailed activity data and local measurements. The uncertainties for emissions from major industrial sectors, such as ferrous metal manufacturing, non-ferrous metal manufacturing, and non-metallic mineral manufacturing, were

significantly improved by the detailed emission estimation approach for the different process segments. However, large uncertainties remained for emissions from chemical manufacturing due to the many uncategorized processes and emissions for that sector. The uncertainties for emissions from vehicles and non-road machinery in this study were mainly from the activity data. Although their population could be obtained from the statistical yearbooks, VMT and working hours could not be estimated accurately. Dust emissions from construction and roads dust had much higher uncertainties as their activity data lacked detail and fewer EFs were available. Most of the area sources, such as residential and agricultural, were estimated from activity data obtained from the statistical yearbooks, resulting in higher uncertainties in their emission estimates. Despite these limitations, the emission estimation approach, based on refined process segments and local measurements, reduced the overall uncertainties of the EI. However, more comprehensive activity data and accurate EFs are still required to improve the quality of EIs in the future.

Table 3. Uncertainty assessment for the major emission sources in the YRD region.

Sources	SO_2	NOx	CO	NMVOCs	PM_{10}	$PM_{2.5}$	NH_3
Power plants	(-25%, 28%)	(-33%, 15%)	(-26%, 27%)	(-28%, 22%)	(-24%, 29%)	(-25%, 28%)	(-45%, 76%)
Boilers	(-29%, 38%)	(-23%, 27%)	(-24%, 30%)	(-19%, 23%)	(-24%, 30%)	(-24%, 30%)	(-46%, 56%)
Petroleum refining	(-49%, 84%)	(-45%, 72%)	(-51%, 90%)	(-40%, 57%)	(-53%, 60%)	(-53%, 64%)	(-39%, 62%)
Chemical manufacturing				(-71%, 167%)			
Ferrous metal manufacturing				(-41%, 61%)	(-23%, 48%)	(-12%, 34%)	
Non-ferrous metal manufacturing	(-37%, 78%)	(-42%, 62%)		(-44%, 70%)	(-38%, 60%)	(-52%, 94%)	
Non-metallic mineral manufacturing	(-48%, 75%)	(-46%, 71%)	(-47%, 72%)	(-45%, 69%)	(-44%, 74%)	(-43%, 68%)	
Vehicles		(-38%, 55%)	(-48%, 73%)	(-46%, 69%)	(-50%, 83%)	(-44%, 67%)	(-55%, 98%)
Non-road machinery	(-47%, 75%)	(-44%, 66%)	(-57%, 112%)	(-50%, 86%)	(-46%, 76%)	(-45%, 77%)	
Construction dust					(-56%, 104%)	(-57%, 102%)	
Road dust					(-35%, 71%)	(-43%, 68%)	
Oil storage and transportation sources				(-43%, 69%)			
Residential solvent-use				(-57%, 116%)			
Residential combustion	(-64%, 143%)	(-44%, 79%)	(-70%, 88%)	(-68%, 165%)	(-43%, 66%)	(-43%, 66%)	(-44%, 72%)
Biomass burning	(-66%, 171%)	(-62%, 124%)	(-67%, 153%)	(-65%, 142%)	(-66%, 149%)	(-66%, 152%)	(-68%, 159%)
Livestock and poultry farming							(-67%, 148%)
Fertilizer application							(-78%, 213%)
Overall	(-29%, 36%)	(-28%, 33%)	(-42%, 75%)	(-44%, 68%)	(-36%, 62%)	(-30%, 46%)	(-58%, 117%)

562 3.2 $PM_{2.5}$ and NMVOC species emissions

563 3.2.1 $PM_{2.5}$ species

564 Figure 6 shows the major source contributions and species comprising $PM_{2.5}$ in
565 the EI. OC, Ca, Si, PSO_4, and EC were top five components of primary $PM_{2.5}$ in the
566 YRD region, accounting for 9.0%, 7.0%, 6.4%, 4.6%, and 4.3% of $PM_{2.5}$ emissions
567 respectively. There were large differences in the emission contributions for the different
568 $PM_{2.5}$ species. Among the industrial sources, the non-metallic mineral manufacturing
569 sector made the largest contributions to Ca, Si, and Al emissions, accounting for 51.6%,
570 15.9%, and 18.8% of these species respectively. Ferrous metal manufacturing was the
571 main source of Fe emissions, accounting for 57.9%. Vehicles were major contributors
572 to OC and EC emissions at 18.0% and 43.5% respectively. K and Cl emissions mainly
573 came from biomass burning, accounting for 50.4% and 78.5% respectively.
574 Construction dust was also an important source of $PM_{2.5}$ species, accounting for 15.9%,
575 34.1% and 20.4% of Ca, Si, and Al emissions respectively.
576

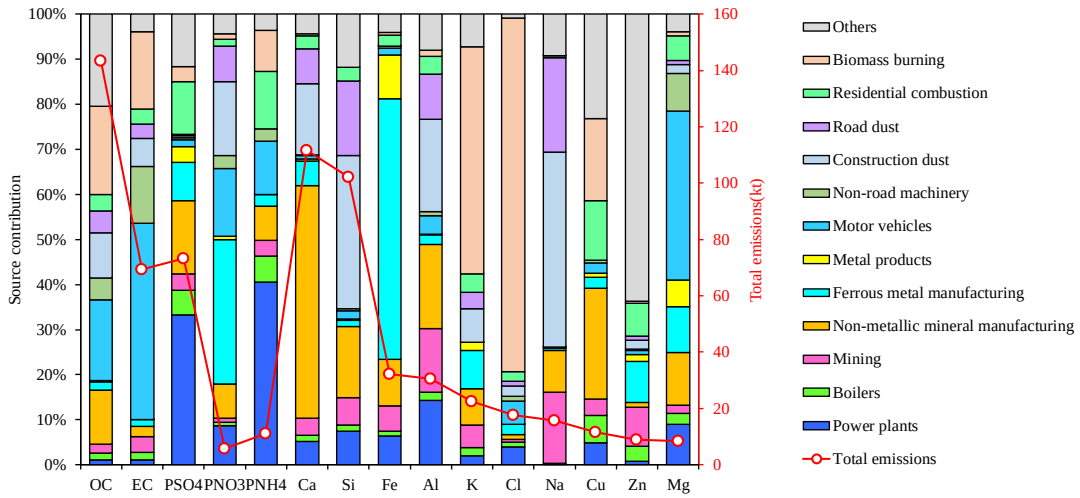

577
578 **Figure 6.** Major source contributions and species comprising $PM_{2.5}$ in the YRD region.
579

580 3.2.2 NMVOC species

581 Figure 7 shows the major source contributions for species comprising NMVOC.
582 Aromatic hydrocarbons and alkanes were the main NMVOC species, accounting for
583 ~25% each of the total NMVOC emissions in the YRD region. Among the alkanes, the

584 linear, branched, and cycloalkanes made up 11.9%, 9.9%, and 2.8% of the total
585 respectively. OVOCs also accounted for a considerable proportion (21.9%) of NMVOC
586 emissions in the YRD region. Among these, aldehydes, ketones, alcohols and esters
587 made up 5.0%, 4.4%, 9.0% and 3.5% of the total respectively. Haloalkanes accounted
588 for 3.1% of the total NMVOC emissions. In the previous study of NMVOC emissions
589 in the YRD region by Wu et al. (2017), aromatic hydrocarbons were also the dominant
590 species (40%), concentrations of OVOCs were similar, while the proportion of alkenes
591 and haloalkanes were generally lower.

592 Chemical manufacturing accounted for a considerable proportion of various
593 NMVOC species in the YRD region, accounting for 12.7%, 21.5%, 13.7%, and 10.8%
594 of the alkane, alkene, aromatic hydrocarbon, and OVOC emissions respectively.
595 Industrial solvent-use sources, which included furniture and wood processing, textiles,
596 packaging and printing, pharmaceutical manufacturing, metal products, auto
597 manufacturing, and appliance manufacturing, were also an important source of
598 NMVOC emissions in this region. Industrial solvent-use sources accounted for 29.3%
599 and 33.3% of aromatic hydrocarbon and OVOC emissions respectively, while
600 residential solvent-use sources accounted for 23.7% and 4.9% of aromatic hydrocarbon
601 and OVOC emissions respectively. Motor vehicles also made a significant contribution
602 to NMVOC species in the YRD region, making up 31.2%, 10.4%, 15.1%, and 10.5%
603 of the total emissions of alkanes, alkenes, aromatics, and OVOC in the region
604 respectively. Biomass burning contributed to 12.0% of aldehyde emissions, although it
605 accounted for only 2.5% of the total NMVOC emissions in the region.

606 Overall, the refinement of the source profiles helped to assess the impact of
607 NMVOC emissions on ambient air quality in the region. However, differences in
608 NMVOC compositions between studies remained and efforts should be made to
609 improve the verification of NMVOC species in future emissions studies.

610

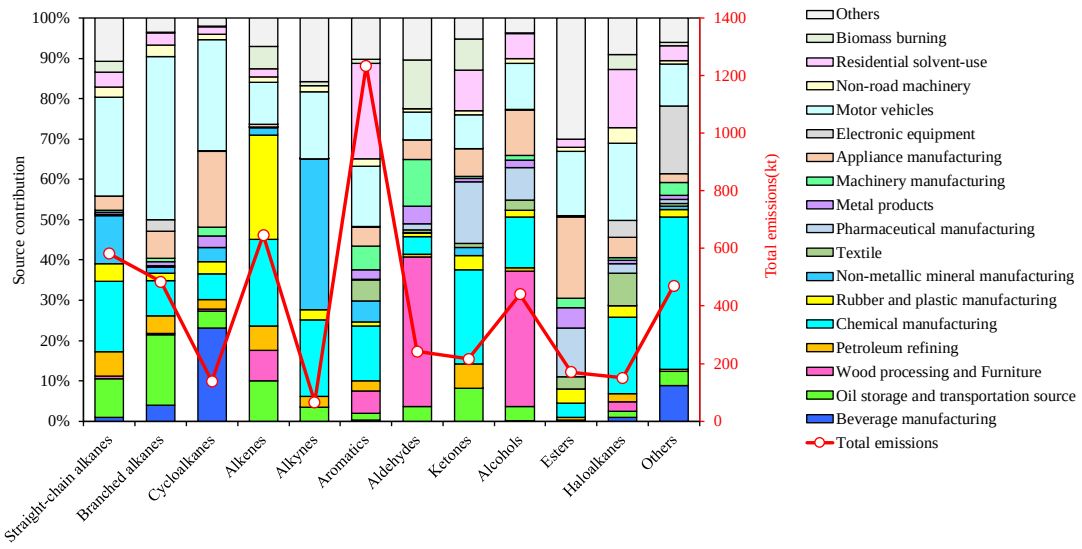

Figure 7. Major source contributions of species comprising NMVOC in the YRD region.

3.3 Model validation

Figure 8 shows a comparison of the simulated and observed concentrations for SO_2, NO_2, $PM_{2.5}$, PM_{10}, O_3, and CO for cities in the YRD region in January and July 2017. The simulated concentration distribution of the different pollutants was consistent with the observed results, indicating that the updated EI generally reflected the distribution of air pollution sources in the YRD region. Comparatively, agreement between the simulated concentration distribution and the observed results for the cities in the central areas of the YRD region was stronger than cities of the northern and southern border areas. This was mainly because border areas were more susceptible to the effects of emissions from areas outside the region, which resulted in greater deviation of the simulation results. A statistical analysis of the hourly concentrations obtained from the model for the pollutants in each city can be found in Table S7 of the supporting information. Figure 9 shows the mean fractional error (MFE) and the mean fractional bias (MFB) between the simulated and observed daily average concentrations in the cities of the region. Overall, the MFB and MFE of simulation and observation results of all the pollutants in January and July were all within the criteria (MFB $\leq \pm 60\%$, MFE $\leq 75\%$) of model performance recommended by Boylan and Russell (2006), and

most of them were with the performance goals (MFB ≤ ±30%, MFE ≤ 50%), which indicated that the EI in this study could reflect the air pollution in winter in the YRD region. In July, the MFB and MFE of O_3 and $PM_{2.5}$ model performance all fell within the criteria range. However, the simulation results of primary pollutants like SO_2, NO_2, PM_{10} and CO were somewhat underestimated. Especially for SO_2 and CO, nearly half of the cities had MFBs lower than -60%, and the cities with large deviations were mainly concentrated in peripheral areas of the YRD region (such as Huangshan, Chizhou, Xuancheng, Lishui, etc.). These cities generally had higher contributions of area emissions from residential and agriculture sources instead of large point industrial sources. The activity data of these sources usually had higher uncertainties and would easily cause the deviation of emission estimation. For example, the underestimation of the amount of residential coal combustion would undoubtedly lead to a severely low estimate of SO_2 and CO emissions. However, since $PM_{2.5}$ and O_3 pollution were more regional, their simulation results were less affected by insufficient local activity data in these cities. Conducting more detailed on-site investigations to obtain more accurate activity data is the key to further improving the performance of EI in the future.

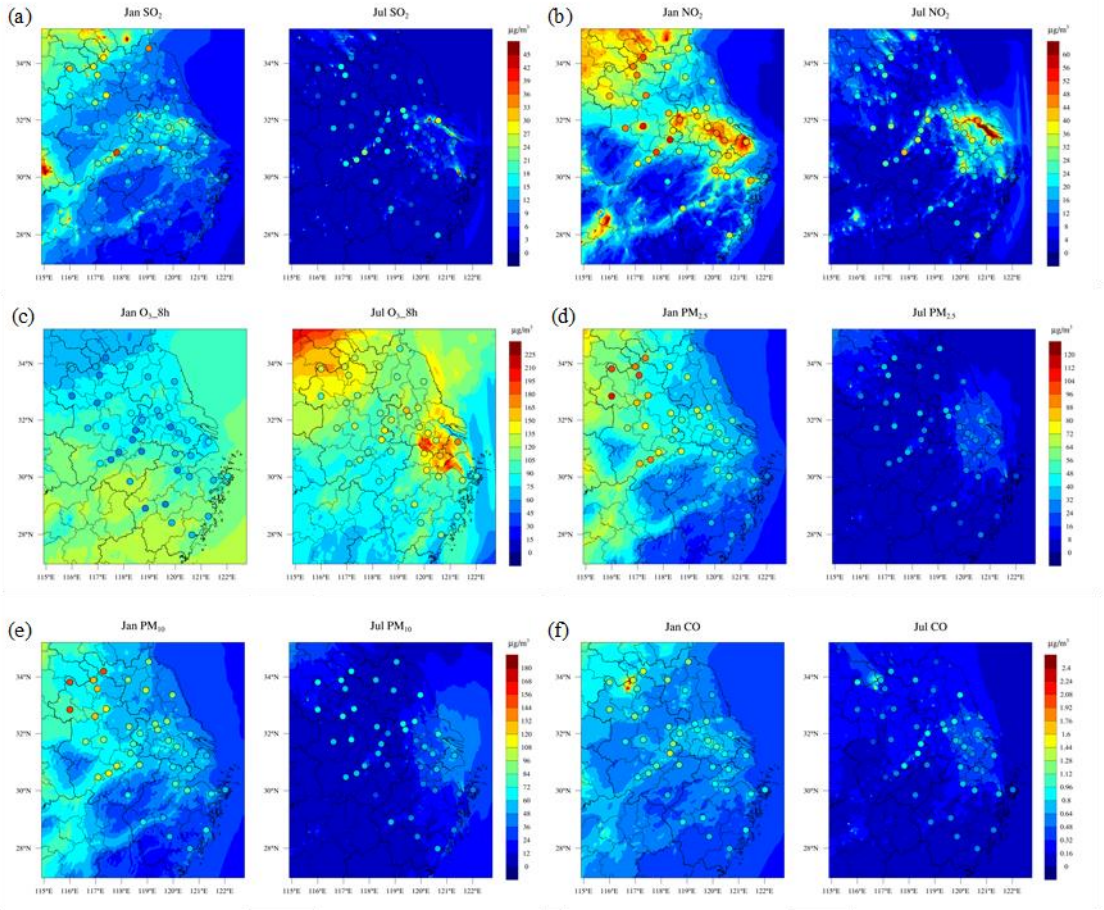

Figure 8. Comparisons of simulated and observed (circles) monthly average pollutant concentrations for cities in the YRD region in January and July 2017: (a) SO_2; (b) NO_2; (c) daily maximum 8-hour O_3 (O_3_8h); (d) $PM_{2.5}$; (e) PM_{10}; and (f) CO.

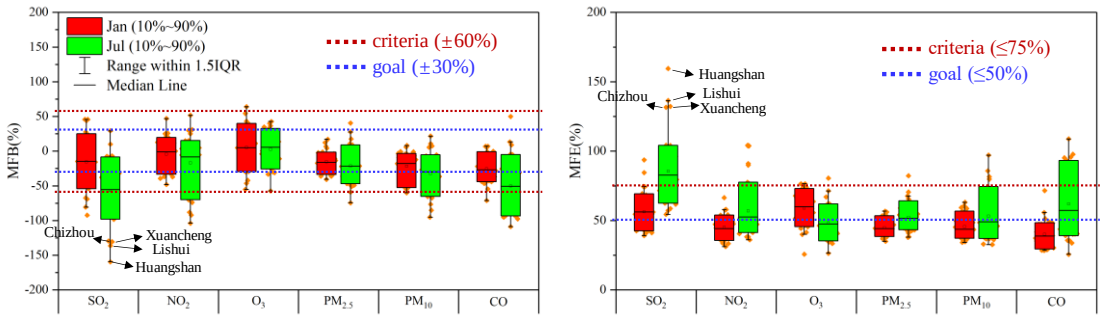

Figure 9. MFB (a) and MFE (b) between the simulation and observation data for daily average concentrations of various pollutants of the cities in the YRD region in January and July 2017

3.4 Ozone and SOA formation potentials

Figure 9 shows the OFP and SOAP contributions for major NMVOC species, emission sources, and industrial sectors in the region. Toluene was the most important NMVOC species for both OFP and SOAP and contributed to 45.0% of the total (7.5%

OFP and 37.5% SOAP), followed by 1,2,4-trimethylbenzene which contributed to 29.1% of the total (2.1% OFP and 27.0% SOAP). Other NMVOC included m/p-xylene, propylene, ethene, o-xylene, ethylbenzene which gave combined contributions to OFP and SOAP of 14.9%, 16.6%, 10.7%, 5.7%, and 2.7% respectively; OFP was the major contribution.

Industrial process sources had the highest OFP and SOAP in the region contributing 44.9% and 26.7% respectively. Industrial solvent-use sources followed, with OFP and SOAP contributions of 15.0% and 33.8%; their contribution to SOAP exceeded that of the industrial process sources. The contribution of motor vehicles to regional OFP and SOAP were 13.9% and 13.5% respectively, which was close to those from residential solvent-use sources. These two sources were the major contributors to O_3 and SOA formation in urban areas.

Four major industrial sectors could account for most of the OFP and SOAP in the YRD region: The chemical manufacturing sector contributed 16.4% and 14.8% to OFP and SOAP respectively; the rubber & plastic manufacturing sector had a SOAP contribution rate of 11.8% (its OFP was relatively low at 1.2%); the appliance manufacturing and textile sectors, accounted for 10.5% and 10.4% of OFP and SOAP contributions respectively.

Based on the above, it was concluded that the reduction of aromatic hydrocarbon emissions from industrial and vehicular sources were of greatest importance for the YRD region. In particular, the high reactivity species, such as toluene, xylene, and trimethylbenzene should be given priority in NMVOCs pollution control measures for the region.

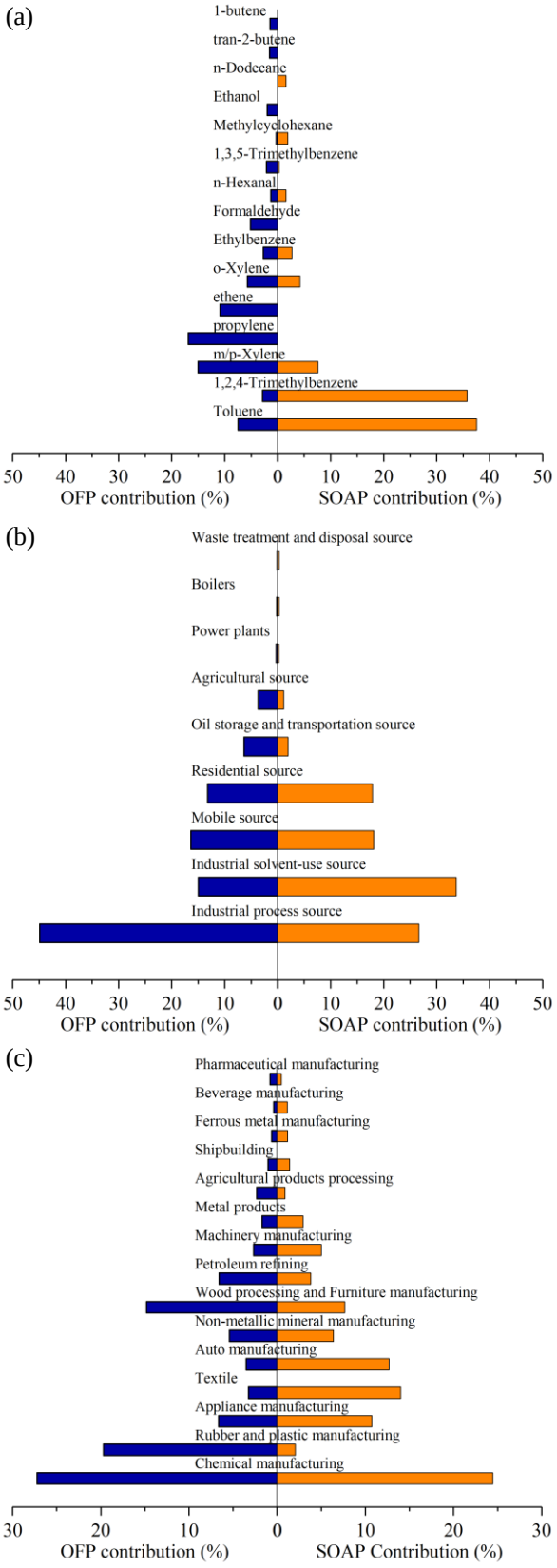

Figure 10. OFP and SOAP formation potentials for different variables: (a) NMVOC species; (b) emission sources; and (c) industrial sectors.

4. Conclusions

A high-resolution air pollutant EI for the YRD region was updated using EFs derived mainly from local measurements. In addition to the conventional pollutants, 424 NMVOCs and 43 $PM_{2.5}$ components were also included in the inventory. The EI was refined into four main categories comprising 259 specific sources. The results indicated that the total emissions of SO_2, NO_x, CO, NMVOCs, PM_{10}, $PM_{2.5}$, and NH_3 in the YRD region in 2017 were 1,552, 3,235, 38,507, 4,875, 3,770, 1,597, and 2,467 Gg, respectively. Overall, SO_2 and NO_x emissions estimated in this study were lower than the previous EIs such as the MEIC. Substantial reductions in emissions from power plants and boilers in recent years were a significant factor. The NMVOC emissions were also slightly lower than the results of previous studies. This was mainly due the use of EFs refined to the specific sectors in this study, which were generally lower than the comprehensive EFs used elsewhere. PM_{10} and $PM_{2.5}$ emissions were respectively 1.7 times and 0.5 times higher than the MEIC, due to the inclusion of dust sources. The NH_3 emissions from this study, estimated using localized EFs, were significantly higher than those of previous studies.

SO_2 and CO emissions were mainly from boilers in the region, accounting for 49% and 73% of the total. Mobile sources dominated NO_x emissions from anthropogenic sources, accounting for 57% of the total. NMVOC emissions were mostly from industrial sources, accounting for 61% of the total. The main contributing industrial sectors were chemical manufacturing and solvent-use sources like furniture manufacturing, appliance manufacturing, textiles, packaging and printing, and machinery manufacturing. Dust sources were responsible for 55% and 28% of PM_{10} and $PM_{2.5}$, respectively. Agricultural sources accounted for 91% of NH_3 emissions.

The main $PM_{2.5}$ species emitted from anthropogenic sources in the YRD region were OC, Ca, Si, PSO_4 and EC, which accounted for 9.0%, 7.0%, 6.4%, 4.6% and 4.3% of total primary $PM_{2.5}$ emissions respectively. The main species of NMVOCs are aromatic hydrocarbons, accounting for 25.3% of the total. OVOCs also made up a

relatively high proportion of NMVOC, accounting for 21.9% of the total. Among these, aldehydes, ketones, alcohols, and esters accounted for 5.0%, 4.4%, 9.0% and 3.5% respectively. Toluene had the highest OFP and SOAP while other contributors included 1,2,4-trimethylbenzene, m,p-xylene, propylene, ethene, o-xylene, ethylbenzene. Industrial process and solvent use sources were the main sources of OFP and SOAP followed by motor vehicles. Among the industrial sources, chemical manufacturing, rubber & plastic manufacturing, appliance manufacturing and textiles all made significant contributions.

In recent years, the ambient air quality in the YRD region has improved significantly. At the same time, contributions to air pollutants from emissions have changed subtly. While emissions of primary pollutants such as SO_2 and NO_x from power plants and boilers have decreased significantly, the contribution from mobile sources have become important. Furthermore, emissions of reactive organic compounds from industrial sources were still at a high level, resulting in elevated secondary pollution issues. The high-resolution EI established in this study should provide scientific guidance for the future control of air pollutants in the YRD region of China.

Acknowledgement

This work was supported by the National Natural Science Foundation of China (Grant No. 21777101; 21677038), the National Key R&D Program of China (Grant No. 2018YFC0213800), and the Shanghai Municipal Bureau of Ecology and Environment Fund Project (Grant No. 2019-01).

Data availability

The gridded emissions of air pollutants from various sources for the YRD region developed by this study at a horizontal resolution of 4 × 4km and a summary table of emissions by cities and sources can be downloaded from website (https://doi.org/10.6084/m9.figshare.13340648). Additional related data is available upon request by contacting the corresponding author (Cheng Huang; huangc@saes.sh.cn).

Author contribution

C.H., H.W. and C.C. designed the research. J.A., Y.H., X.W., R.Y., Q.W., Y.L., and C.X. performed the research. H.W. and S.J. collected the NMVOC species data. L.Q., M.Z., and S.Z. collected the $PM_{2.5}$ species data. C.H., Q.H., and J.L. supported the emission factor data. J.A., Y.H., C.H., X.W., H.L., Y.Z., Y.C., and C.C. analyzed the results. J.A., Y.H, C.H., and X.W. wrote the paper.

Competing interests

The authors declare that they have no conflict of interest.

References

Boylan, J. W., and Russell, A. G.: PM and light extinction model performance metrics, goals, and criteria for three-dimensional air quality models, Atmos. Environ., 40, 4946-4959, 2006.

Cai, S. Y., Ma, Q., Wang, S. X., Zhao, B., Brauer, M., Cohen, A., Marting, R. V., Zhang, Q. Q., Li, Q. B., Wang, Y. X., Hao, J. M., Frostad, J., Forouzanfar, M. H., and Burnettk, R. T.: Impact of air pollution control policies on future $PM_{2.5}$ concentrations and their source contributions in China, J. Environ. Manage., 227, 124–133, 2018.

Carter, W. P. L.: Development of ozone reactivity scales for volatile organic compounds, J. Air Waste Manage. Assoc., 44, 881–899, 1994.

Chen, Y.: Study on characteristics ammonia emission from typical large scale pig farm in Shanghai, Master Thesis, East China University of Science and Technology, 2017 (in Chinese).

Chen, Y., Fang, X. F., Shen, G. X., Xu, C., Qian, X. Y., Zhao, Z. G., Yu, S. F., Li, J. W., and Wang, Z. Q.: Research on ammonia emission characteristics and its influencing factors from paddy fields in Taihu Lake region, Acta Agriculturae Zhejiangensis, 29, 119−128, 2017 (in Chinese).

Crippa, M., Guizzardi, D., Muntean, M., Schaaf, E., Dentener, F., van Aardenne, J. A., Monni, S., Doering, U., Olivier, J. G. J., Pagliari, V., and Janssens-Maenhout, G.: Gridded emissions of air pollutants for the period 1970–2012 within EDGAR v4.3.2, Earth Syst.

769 Sci. Data, 10, 1987–2013, 2018.
770 Emery, C., Liu, Z., Russell, A. G., Odman, M. T., Yarwood, G., and Kumar, N.:
771 Recommendations on statistics and benchmarks to assess photochemical model
772 performance, J. Air Waste Manag. Assoc., 67, 582-598, 2017.
773 European Environment Agency (EEA): EMEP/EEA air pollution emission inventory
774 guidebook, http://www.eea.europa.eu/publications/emep-eea-emission-inventory-
775 guidebook-2013, 2013.
776 Fan, Q. Z., Zhang, Y., Ma, W. C., Ma, H. X., Feng, J. L., Yu, Q., Yang, X., Ng, S. K. W., Fu, Q.
777 Y., and Chen, L. M.: Spatial and seasonal dynamics of ship emissions over the Yangtze
778 River Delta and East China Sea and their potential environmental influence, Environ. Sci.
779 Technol., 50, 1322−1329, 2016.
780 Fiore, A. M., Naik, V., Spracklen, D. V., Steiner, A., Unger, N., Prather, M., Bergmann, D.,
781 Cameron-Smith, P. J., Cionni, I., Collins, W. J., Dalsøren, S., Eyring, V., Folberth, G. A.,
782 Ginoux, P., Horowitz, L. W., Josse, B., Lamarque, J., MacKenzie, I. A., Nagashima, T.,
783 O'Connor, F. M., Righi, M., Rumbold, S. T., Shindell, D. T., Skeie, R. B., Sudo, K., Szopa,
784 S., Takemurat, T., and Zeng, G.: Global air quality and climate, Chem. Soc. Rev., 41, 6663–
785 6683, 2012.
786 Fu, M. L., Ge, Y. S., Tan, J. W., Zeng, T., and Liang, B.: Characteristics of typical non-road
787 machinery emissions in China by using portable emission measurement system, Sci. Total
788 Environ., 437, 255–261, 2012.
789 Fu, M. L., Ding, Y., Yin, H., Ji, Z., Ge, Y. S., and Liang, B.: Characteristics of agricultural
790 tractors emissions under real-world operating cycle, Transactions of the Chinese Society
791 of Agricultural Engineering, 29, 42–48, 2013 (in Chinese).
792 Fu, X., Wang, S. X., Zhao, B., Xing, J., Cheng, Z., Liu, H., and Hao, J. M.: Emission inventory
793 of primary pollutants and chemical speciation in 2010 for the Yangtze River Delta region,
794 China, Atmos. Environ., 70, 39–50, 2013.
795 Gao, Y. Q., Wang, H. L., Xu, R. Z., Jing, S. A., Liu, Y. H., and Peng, Y. R.: Characterization of
796 volatile organic compounds from cooking emissions, Huanjing Kexue, 40, 1627–1633,

2019 (in Chinese).

Ge, Y. S., Liu, H. K., Ding, Y., Yin, H., Fu, M. L., and Li, J. Q.: Experimental study on characteristics of emissions and fuel consumption for combines, Transactions of the Chinese Society of Agricultural Engineering, 29, 41–47, 2013 (in Chinese).

Guan, W. J., Zheng, X. Y., Chung, K. F., and Zhong, N. S.: Impact of air pollution on the burden of chronic respiratory diseases in China: time for urgent action, Lancet, 388, 1939–1951, 2016.

Guo, Y. Y., Gao, X., Zhu, T. Y., Luo, L., and Zheng, Y.: Chemical profiles of PM emitted from the iron and steel industry in northern China, Atmos. Environ., 150, 187–197, 2017.

Hoesly, R. M., Smith, S. J., Feng, L., Klimont, Z., Janssens-Maenhout, G., Pitkanen, T., Seibert, J. J., Vu, L., Andres, R. J., Bolt, R. M., Bond, T. C., Dawidowski, L., Kholod, N., Kurokawa, J. I., Li, M., Liu, L., Lu, Z., Moura, M. C. P., O'Rourke, P. R., and Zhang, Q.: Historical (1750–2014) anthropogenic emissions of reactive gases and aerosols from the Community Emissions Data System (CEDS), Geosci. Model Dev., 11, 369–408, 2018.

Huang, C., Chen, C. H., Li, L., Cheng, Z., Wang, H. L., Huang, H. Y., Streets, D. G., Wang, Y. J., Zhang, G. F., and Chen, Y. R.: Emission inventory of anthropogenic air pollutants and VOC species in the Yangtze River Delta region, China, Atmos. Chem. Phys., 11, 4105–4120, 2011.

Huang, C., Wang, H. L., Li, L., Wang, Q., Lu, Q., de Gouw, J. A., Zhou, M., Jing, S. A., Lu, J., and Chen, C. H.: VOC species and emission inventory from vehicles and their SOA formation potentials estimation in Shanghai, China, Atmos. Chem. Phys., 15, 11081–11096, 2015.

Huang, C., Lou, S. R., Qiao, L. P., Jing, S. A., Tao, S. K., Zhou, M., and Chen, C. H.: Physicochemical characteristics of real-world PM emissions from heavy-duty diesel buses, Research of Environmental Sciences, 29, 1352–1361, 2016 (in Chinese).

Huang, C., Tao, S. K., Lou, S. R., Hu, Q. Y., Wang, H. L., Wang, Q., Li, L., Wang, H. Y., Liu, J. G., Quan, Y. F., and Zhou, L. L.: Evaluation of emission factors for light-duty gasoline vehicles based on chassis dynamometer and tunnel studies in Shanghai, China, Atmos.

825 Environ., 169, 193–203, 2017.
826 Huang, C., An, J. Y., and Lu, J.: Emission inventory and prediction of non-road machineries in
827 the Yangtze River Delta region, China, Huanjing Kexue, 39, 3965–3975, 2018a (in
828 Chinese).
829 Huang, C., Hu, Q. Y., and Lu, J.: Measurements of OC and EC emission factors for light-duty
830 gasoline vehicles, Huanjing Kexue, 39, 3110–3117, 2018b (in Chinese).
831 Huang, C., Hu, Q. Y., Lou, S. R., Tian, J. J., Wang, R. N., Xu, C., An, J. Y., Ren, H. J., Ma, D.,
832 Quan, Y. F., Zhang, Y. J., and Li, L.: Ammonia emission measurements for light-duty
833 gasoline vehicles in China and implications for emission modeling, Environ. Sci. Technol.,
834 52, 11223−11231, 2018c.
835 Huang, C., Hu, Q. Y., Wang, H. Y., Qiao, L. P., Jing, S. A., Wang, H. L., Zhou, M., Zhu, S. H.,
836 Ma, Y. G., Lou, S. R., Li, L., Tao, S. K., Li, Y. J., and Lou, D. M.: Emission factors of
837 particulate and gaseous compounds from a large cargo vessel operated under real-world
838 conditions, Environ. Pollut., 242, 667−674, 2018d.
839 Hsu, Y., Divita, F., and Dorn, J.: SPECIATE version 4.4 database development documentation,
840 final report, EPA/600/R-13/307, 2014.
841 International Civil Aviation Organization (ICAO): ICAO Environmental Report 2013,
842 Montreal, Canada, 2014.
843 Janssens-Maenhout, G., Crippa, M., Guizzardi, D., Dentener, F., Muntean, M., Pouliot, G.,
844 Keating, T., Zhang, Q., Kurokawa, J., Wankmüller, R., Denier van der Gon, H., Kuenen,
845 J. J. P., Klimont, Z., Frost, G., Darras, S., Koffi, B., and Li, M.: HTAP_v2.2: a mosaic of
846 regional and global emission grid maps for 2008 and 2010 to study hemispheric transport
847 of air pollution, Atmos. Chem. Phys., 15, 11411–11432, 2015.
848 Jing, S. A., Wang, H. L., Zhu, H. L., Yang, Q., Lu, B., Xia, Y., Yu, C. G., Tao, S. K., Li, L., Lou,
849 S. R., Huang, C., Tang, W., and Jing, B. L.: Treatment status and emission characteristics
850 of volatile organic compounds from typical industrial sources, Huanjing Kexue, 39, 3091–
851 3095, 2018 (in Chinese).
852 Klimont, Z., Kupiainen, K., Heyes, C., Purohit, P., Cofala, J., Rafaj, P., Borken-Kleefeld, J., and

Schöpp, W.: Global anthropogenic emissions of particulate matter including black carbon, Atmos. Chem. Phys., 17, 8681–8723, 2017.

Li, L., An, J. Y., Zhou, M., Qiao, L. P., Zhu, S. H., Yan, R. S., Ooi, C. G., Wang, H. L., Huang, C., Huang, L., Tao, S. K., Yu, J. Z., Chan, A., Wang, Y. J., Feng, J. L., Chen, C. H.: An integrated source apportionment methodology and its application over the Yangtze River Delta region, China, Environ. Sci. Technol., 52, 14216−14227, 2018.

Li, L., An, J. Y., Huang, L., Yan, R. S., Huang, C., Yarwood, G.: Ozone source apportionment over the Yangtze River Delta region, China: Investigation of regional transport, sectoral contributions and seasonal differences, Atmos. Environ., 202, 269–280, 2019.

Li, M., Zhang, Q., Streets, D. G., He, K. B., Cheng, Y. F., Emmons, L. K., Huo, H., Kang, S. C., Lu, Z., Shao, M., Su, H., Yu, X., and Zhang, Y.: Mapping Asian anthropogenic emissions of non-methane volatile organic compounds to multiple chemical mechanisms, Atmos. Chem. Phys., 14, 5617–5638, 2014.

Li, Z., Zhang, K.S., Pang, K.L., and Di, B.F.: A fuel-based approach for emission factor development for highway paving construction equipment in China, J. Air Waste Manage. Assoc., 66, 1214–1223, 2016.

Liang, C. S., Duan, F. Q., He, K. B., and Ma, Y. L.: Review on recent progress in observations, source identifications and countermeasures of $PM_{2.5}$, Environ. Int., 86, 150–170, 2016.

Liu, Z. Q.: Study on the estimation of NO_x from thermal power industry in China, Master thesis, North China Electric Power University, China, Beijing, 2008 (in Chinese).

Lu, J., Huang, C., Hu, Q. Y., Yang, Q., Jing, B. L., Xia, Y., Lu, B., Tang, W., Lou, S. R., Tao, S. K., and Li, L.: Air pollutant emissions inventory of non-road machinery in typical cities in Eastern China, Huanjing Kexue, 38, 2738–2746, 2017 (in Chinese).

Lou, S. R.: Emission characteristics of $PM_{2.5}$ from medium and small capacity coal-fired boilers in service, Acta Scientiae Circumstantiae, 34, 3119–3125, 2014 (in Chinese).

Ministry of Environmental Protection (MEP), P.R. of China: Guidebooks for compiling air pollution emission inventories. Available via. http://www.zhb.gov.cn/gkml/hbb/bgg/201408/t20140828_288364.htm, 2014 (in Chinese).

881 Monks, P. S., Granier, C., Fuzzi, S., Stohl, A., Williams, M. L., Akimoto, H., Amann, M.,
882 Baklanov, A., Baltensperger, U., Bey, I., Blake, N., Blake, R. S., Carslaw, K., Cooper, O.
883 R., Dentener, F., Fowler, D., Fragkou, E., Frost, G. J., Generoso, S., Ginoux, P., Grewe, V.,
884 Guenther, A., Hansson, H. C., Henne, S., Hjorth, J., Hofzumahaus, A., Huntrieser, H.,
885 Isaksen, I. S. A., Jenkin, M. E., Kaiser, J., Kanakidou, M., Klimont, Z., Kulmala, M., Laj,
886 P., Lawrence, M. G., Lee, J. D., Liousse, C., Maione, M., McFiggans, G., Metzger, A.,
887 Mieville, A., Moussiopoulos, N., Orlando, J. J., O'Dowd, C. D., Palmer, P. I., Parrish, D.
888 D., Petzold, A., Platt, U., Pöschl, U., Prévôt, A. S. H., Reeves, C. E., Reimann, S., Rudich,
889 Y., Sellegri, K., Steinbrecher, R., Simpson, D., ten Brink, H., Theloke, J., van derWerf, G.
890 R., Vautard, R., Vestreng, V., Vlachokostas, C., and von Glasow, R.: Atmospheric
891 composition change – global and regional air quality, Atmos. Environ., 43, 5268–5350,
892 2009.
893 National Bureau of Statistics of China: China Statistical Yearbook 2018. China Statistics Press,
894 Beijing, 2018
895 Ni, Z., Luo, K., Gao, Y., Gao, X., Jiang, F., Huang, C., Fan, J., Fu, J., and Chen, C.: Spatial–
896 temporal variations and process analysis of O_3 pollution in Hangzhou during the G20
897 summit, Atmos. Chem. Phys., 20, 5963–5976, 2020.
898 Qiao, L. P., Cai, J., Wang, H. L., Wang, W. B., Zhou, M., Lou, S. R., Chen, R. J., Dai, H. X.,
899 Chen, C. H., and Kan, H. D.: $PM_{2.5}$ constituents and hospital emergency-room visits in
900 Shanghai, China, Environ. Sci. Technol., 48, 10406−10414, 2014.
901 Qu, L., He, L. Q., Hu, J. N., Jin, T. S., Zu, L., Wang, M. Y., and Song, J. H.: Characteristics of
902 $PM_{2.5}$ emissions and its carbonaceous components from construction machines under
903 different typical driving modes, Research of Environmental Sciences, 28, 1047–1052,
904 2015 (in Chinese).
905 Reff, A., Bhave, P. V., Simon, H., Pace, T. G., Pouliot, G. A., Mobley, J. D., and Houyoux, M.:
906 Emissions inventory of $PM_{2.5}$ trace elements across the United States, Environ. Sci.
907 Technol., 43, 5790–5796, 2009.
908 Requia, W. J., Adams, M. D., Arain, A., Papatheodorou, S., Koutrakis, P., and Mahmoud, M.:

909 Global association of air pollution and cardiorespiratory diseases: a systematic review,
910 meta-Analysis, and investigation of modifier variables. Am. J. Public Health, 108, S123–
911 S130, 2018.
912 Sha, T., Ma, X. Y., Jia, H. L., van der A, R. J., Ding, J. Y., Zhang, Y. L., Chang, Y. H.: Exploring
913 the influence of two inventories on simulated air pollutants during winter over the Yangtze
914 River Delta, Atmos. Environ., 206, 170–182, 2019.
915 Simayi, M., Hao, Y. F., Li, J., Wu, R. R., Shi, Y. Q., Xi, Z. Y., Zhou, Y., Xie, S. D.: Establishment
916 of county-level emission inventory for industrial NMVOCs in China and spatial-temporal
917 characteristics for 2010–2016, Atmos. Environ., 211, 194–203, 2019.
918 Song, C. B., Ma, C., Zhang, Y. J., Wang, T., Wu, L., Wang, P., Liu, Y., Li, Q., Zhang, J. S., Dai,
919 Q. L., Zou, C., Sun, L. N., Mao, H. J.: Heavy-duty diesel vehicles dominate vehicle
920 emissions in a tunnel study in northern China, Sci. Total Environ., 637–638, 431–442,
921 2018.
922 Stroud, C. A., Makar, P. A., Zhang, J. H., Moran, M. D., Akingunola, A., Li, S. M., Leithead,
923 A., Hayden, K., and Siu, M.: Improving air quality model predictions of organic species
924 using measurement-derived organic gaseous and particle emissions in a petrochemical-
925 dominated region, Atmos. Chem. Phys., 18, 13531–13545, 2018.
926 Sun, W., Shao, M., Granier, C., Liu, Y., Ye, C. S., Zheng, J. Y.: Long-Term trends of
927 anthropogenic SO_2, NO_x, CO, and NMVOCs emissions in China, Earth's Future, 6, 1112–
928 1133, 2018a.
929 Sun, X. W., Cheng, S. Y., Lang, J. L., Ren, Z. H., Sun, C.: Development of emissions inventory
930 and identification of sources for priority control in the middle reaches of Yangtze River
931 Urban Agglomerations, Sci. Total Environ., 625, 155–167, 2018.
932 Sun, Y. Y.: Study on emission inventory and uncertainty assessment of multi-pollutants from
933 coal-fired power plants, Master thesis, Zhejiang University, China, Hangzhou, 2015 (in
934 Chinese).
935 Tang, X. B., Huang, C., Lou, S. R., Qiao, L. P., Wang, H. L., Zhou, M., Chen, M. H., Chen, C.
936 H., Wang, Q., Li, G. L., Li, L., Huang, H. Y., and Zhang, G. F.: Emission factors and PM

chemical composition study of biomass burning in the Yangtze River Delta Region, Huanjing Kexue, 35, 1623–1632, 2014 (in Chinese).

U.S. Environmental Protection Agency (USEPA): Compilation of air pollutant emission Factors, AP-42, 5th ed., Washington, DC, 2002.

U.S. Environmental Protection Agency (USEPA): Exhaust and crankcase emission factors for non-road engine modeling-compression ignition, Washington, DC, 2010.

Wang, S., Zhu, F. H., Wang, H. M., Zuo, Y., Sun, X. L., Zhao, X. Y., Chen, H., and Liu, G.: Fine particle emission characteristics from coal-fired power plants based on field test, Acta Scientiae Circumstantiae, 31, 630–635, 2011 (in Chinese).

Wang, J. D., Zhao, B., Wang, S. X., Yang, F. M., Xing, J., Morawska, L., Ding, A. J., Kulmala, M., Kerminen, V., Kujansuu, J., Wang, Z. F., Ding, D., Zhang, X. Y., Wang, H. B., Tian, M., Petäjä, T., Jiang, J. K., and Hao, J. M.: Particulate matter pollution over China and the effects of control policies, Sci. Total Environ., 584–585, 426–447, 2017a.

Wang, H. L., Lou, S. R., Huang, C., Qiao, L. P., Tang, X. B., Chen, C. H., Zeng, L. M., Wang, Q., Zhou, M., Lu, S. H., and Xu, X. N.: Source profiles of volatile organic compounds from biomass burning in Yangtze River Delta, China, Aerosol and Air Quality Research, 14, 818–828, 2014a.

Wang, H. L., Qiao, Y. Z., Chen, C. H., Lu, J., Dai, H. X., Qiao, L. P., Lou, S. R., Huang, C., Li, L., Jing, S. A., and Wu, J. P.: Source profiles and chemical reactivity of volatile organic compounds from solvent use in Shanghai, China, Aerosol and Air Quality Research, 14, 301–310, 2014b.

Wang, H. L., Jing, S. A., Wang, Q., Huang, C., Lou, S. R., Qiao, L. P., and Li, L.: Measurement and characterization of emissions of volatile organic compounds in solvent use, Research of Environmental Sciences, 29, 1433–1439, 2016 (in Chinese).

Wang, H. L., Yang, Z. X., and Jing, S. A.: Volatile organic compounds (VOCs) source profiles of industrial processing and solvent use emissions: a review, Huanjing Kexue, 38, 2617–2628, 2017b (in Chinese).

Wang, H. L., Jing, S. A., Lou, S. R., Hu, Q. Y., Li, L., Tao, S. K., Huang, C., Qiao, L. P., and

965 Chen, C. H.: Volatile organic compounds (VOCs) source profiles of on-road vehicle
966 emissions in China, Sci. Total Environ., 607–608, 253–261, 2017c.
967 Wang, H. L., Jing, S. A., Lou, S. R., Tao, S. K., Qiao, L. P., Li, L., Huang, C., Lin, L., and Chen,
968 C. H.: Estimation of fine particle ($PM_{2.5}$) emission inventory from cooking: case study for
969 Shanghai, Huanjing Kexue, 39, 1971–1977, 2018a (in Chinese).
970 Wang, R. N., Huang, C., Ren, H. J., Yan, R. S., Hong, Z., Xu, C., Hu, Q. Y., An, J. Y., Dong, B.
971 N., and Li, L.: Air pollutant emission inventory from LTO cycles of aircraft in civil aviation
972 airports in the Yangtze River Delta region, China, Acta Scientiae Circumstantiae, 38,
973 4472–4479, 2018b (in Chinese).
974 Wang, P., Ying, Q., Zhang, H. L., Hu, J. L., Lin, Y. C., and Mao, H. J.: Source apportionment
975 of secondary organic aerosol in China using a regional source-oriented chemical transport
976 model and two emission inventories, Environ. Pollut., 237, 756–766, 2018c.
977 Wayson, R. L., Fleming, G. G., and Lovinelli, R.: Methodology to estimate particulate matter
978 emissions from certified commercial aircraft engines, J. Air Waste Manage, 59, 91–100,
979 2009.
980 Wen, Y. F., Wang, H., Larson, T., Kelp, M., Zhang, S. J., Wu, Y., Marshall, J. D.: On-highway
981 vehicle emission factors, and spatial patterns, based on mobile monitoring and absolute
982 principal component score, Sci. Total Environ., 676, 242–251, 2019.
983 Wu, R. R. and Xie, S. D.: Spatial distribution of ozone formation in China derived from
984 emissions of speciated volatile organic compounds, Environ. Sci. Technol., 52, 8146−8156,
985 2018.
986 Wu, R. R. and Xie, S. D.: Spatial distribution of secondary organic aerosol formation potential
987 in China derived from speciated anthropogenic volatile organic compound emissions,
988 Environ. Sci. Technol., 52, 8146−8156, 2018.
989 Wu, R. L., Liu, F., Tong, D., Zheng, Y. X., Lei, Y., Hong, C. P., Li, M., Liu, J., Zheng, B., Bo,
990 Y., Chen, X. T., Li, X., Zhang, Q.: Air quality and health benefits of China's emission
991 control policies on coal-fired power plants during 2005–2020, Environ. Res. Lett., 14,
992 094016, 2019.

Wu, Y., Zhang, S. J., Li, M. L., Ge, Y. S., Shu, J. W., Zhou, Y., Xu, Y. Y., Hu, J. N., Liu, H., Fu, L. X., He, K. B., Hao, J. M.: The challenge to NO_x emission control for heavy-duty diesel vehicles in China, Atmos. Chem. Phys., 12, 9365–9379, 2012.

Xia, Y., Yang, Q., Xu, C., Lu, B., Tang, W., Jing, B. L., Lu, Q., Huang, C., and Lu, J.: Study on high resolution NH_3 emission inventory based on analysis of large data for agriculture in Hangzhou, Acta Scientiae Circumstantiae, 38, 661–668, 2018 (in Chinese).

Xu, J., Huang, C., Li, L., Chen, Y. H., Lou, S. R., Qiao, L. P., and Wang, H. Y.: Chemical composition characteristics of $PM_{2.5}$ emitted by medium and small capacity coal-fired boilers in the Yangtze River Delta Region, Huanjing Kexue, 39, 1493–1501, 2018 (in Chinese).

Yang, Y. and Zhao, Y.: Quantification and evaluation of atmospheric pollutant emissions from open biomass burning with multiple methods: a case study for the Yangtze River Delta region, China, Atmos. Chem. Phys., 19, 327–348, 2019.

Yang, Q., Huang, C., Lu, B., Jing, B. L., Xia, Y., Tang, W., Lu, Q., Lu, J., Xu, C., Gu, Z. Y.: Air pollutant emission inventory based on local emission source surveys in Hangzhou, China, Acta Scientiae Circumstantiae, 37, 3240–3254, 2017 (in Chinese).

Yao, Z. M., Teng, Y., Li, J., Wu, X. F., and Duan, N.: NO_x emission factors from medium and small layer burning boilers firing soft coal, Research of Environmental Sciences, 22, 1263–1268, 2009 (in Chinese).

Ying, Q., Feng, M., Song, D. L., Wu, L., Hu, J. L., Zhang, H. L., Kleeman, M. J., and Li, X. H.: Improve regional distribution and source apportionment of $PM_{2.5}$ trace elements in China using inventory-observation constrained emission factors, Sci. Total Environ., 624, 355–365, 2018.

Zhang, J., Liu, L., Zhao, Y., Li, H., Lian, Y., Zhang, Z., Huang, C., and Du, X.: Development of a high-resolution emission inventory of agricultural machinery with a novel methodology: A case study for Yangtze River Delta region, Environ. Pollut., 266, 115075, 2020.

Zhang, S. J., Wu, Y., Zhao, B., Wu, X. M., Shu, J. W., and Hao, J. M.: City-specific vehicle

emission control strategies to achieve stringent emission reduction targets in China's Yangtze River Delta region, J. Environ. Sci., 51, 75–87, 2017a.

Zhang, X. M., Wu, Y. Y., Liu, X. J., Reis, S., Jin, J. X., Dragosits, U., van Damme, M., Clarisse, L., Whitburn, S., Coheur, P., Gu, B. J.: Ammonia emissions may be substantially underestimated in China, Environ. Sci. Technol., 51, 12089-12096, 2017b.

Zhang, Y., Bo, X., Zhao, Y., Nielsen, C. P.: Benefits of current and future policies on emissions of China's coalfired power sector indicated by continuous emission monitoring, Environ. Pollut., 251, 415–424, 2019.

Zhao, Y., Wang, S. X., Nielsen, C. P., Li, X. H., and Hao, J. M.: Establishment of a database of emission factors for atmospheric pollutants from Chinese coal-fired power plants, Atmos. Environ., 44, 1515–1523, 2010.

Zhao, Y., Qiu, L. P., Xu, R. Y., Xie, F. J., Zhang, Q., Yu, Y. Y., Nielsen, C. P., Qin, H. X., Wang, H. K., Wu, X. C., Li, W. Q., and Zhang, J.: Advantages of a city-scale emission inventory for urban air quality research and policy: the case of Nanjing, a typical industrial city in the Yangtze River Delta, China, Atmos. Chem. Phys., 15, 12623–12644, 2015.

Zhao, Y., Mao, P., Zhou, Y. D., Yang, Y., Zhang, J., Wang, S. K., Dong, Y. P., Xie, F. J., Yu, Y. Y., and Li, W. Q.: Improved provincial emission inventory and speciation profiles of anthropogenic non-methane volatile organic compounds: a case study for Jiangsu, China, Atmos. Chem. Phys., 17, 7733–7756, 2017.

Zhao, Y., Xia, Y. M., Zhou, Y. D.: Assessment of a high-resolution NO_x emission inventory using satellite observations: A case study of southern Jiangsu, China, Atmos. Environ., 190, 135–145, 2018.

Zhao, Y., Yuan, M., Huang, X., Chen, F., and Zhang, J.: Quantification and evaluation of atmospheric ammonia emissions with different methods: a case study for the Yangtze River Delta region, China, Atmos. Chem. Phys., 20, 4275-4294, 2020.

Zheng, B., Zhang, Q., Tong, D., Chen, C., Hong, C., Li, M., Geng, G., Lei, Y., Huo, H., and He, K.: Resolution dependence of uncertainties in gridded emission inventories: a case study in Hebei, China, Atmos. Chem. Phys., 17, 921–933, 2017.

Zheng, B., Tong, D., Li, M., Liu, F., Hong, C. P., Geng, G. N., Li, H. Y., Li, X., Peng, L. Q., Qi, J., Yan, L., Zhang, Y. X., Zhao, H. Y., Zheng, Y. X., He, K. B., and Zhang, Q.: Trends in China's anthropogenic emissions since 2010 as the consequence of clean air actions, Atmos. Chem. Phys., 18, 14095–14111, 2018.

Zheng, H., Cai, S., Wang, S., Zhao, B., Chang, X., and Hao, J.: Development of a unit-based industrial emission inventory in the Beijing–Tianjin–Hebei region and resulting improvement in air quality modeling, Atmos. Chem. Phys., 19, 3447–3462, 2019.

Zheng, J. J., Jiang, P., Qiao, W., Zhu, Y., and Kennedy, E.: Analysis of air pollution reduction and climate change mitigation in the industry sector of Yangtze River Delta in China, J. Clean Prod., 114, 314–322, 2016.

Zheng, M., Zhang, Y. J., Yan, C. Q., Fu, H. Y., Niu, H. Y., Huang, K., Hu, M., Zeng, L. M., Liu, Q. Z., Pei, B., and Fu, Q. Y.: Establishing $PM_{2.5}$ industrial source profiles in Shanghai, China Environmental Science, 33, 1354–1359, 2013 (in Chinese).

Zhou, Y. D., Zhao, Y., Mao, P., Zhang, Q., Zhang, J., Qiu, L. P., and Yang, Y.: Development of a high-resolution emission inventory and its evaluation and application through air quality modeling for Jiangsu Province, China, Atmos. Chem. Phys., 17, 211–233, 2017.

Zhou, Z. Q.: Study on characteristics ammonia emission from typical large scale dairy cow farm in Shanghai, Master Thesis, East China University of Science and Technology, 2019 (in Chinese).